

# ADJACENCY ISSUES IN SOFT-STORY WOOD-FRAME BUILDINGS

A Report To:

Structural Engineers Association of Northern California

By

Bruce Maison,<sup>1</sup> David Bonowitz,<sup>2</sup> Laurence Kornfield,<sup>3</sup> and David McCormick<sup>4</sup>

April 2011

## ABSTRACT

This report presents our results from a computer simulation study on the seismic pounding of soft-story wood-frame buildings. We investigated 1920s era four-story corner buildings that are common in San Francisco, many of which were damaged in the city's Marina District during the 1989 Loma Prieta earthquake. We calibrated two building computer models to simulate actual earthquake response. We then performed computer analysis to assess collapse performance under twenty-two hypothetical pounding situations of both as-built soft-story and retrofitted buildings. For this building type, we found that a *typical* pounding situation increases the collapse rate by 14 percent at design earthquake intensities. For retrofitted versions of the building in a *typical* pounding situation, we found that pounding slightly decreases the collapse rate. However, there were factors that appear to significantly increase the collapse rate especially in combination: negligible building separations, and multiple adjacent buildings having low effective damping and large mass. Based on the results, we outline an approximate way to account for pounding within the context of current design procedures.

---

<sup>1</sup> Structural Engineer, El Cerrito, CA

<sup>2</sup> Structural Engineer, San Francisco, CA

<sup>3</sup> Deputy Director, Department of Building Inspection, City of San Francisco, CA

<sup>4</sup> Principal, Simpson, Gumpertz & Heger, San Francisco, CA

(Intentional blank page)

## CONTENTS

<u>Section</u>	<u>Page</u>
Acknowledgment	4
Introduction	5
San Francisco Soft-Story Buildings	6
Case Study Buildings	8
Building Computer Modeling	11
Building Model Calibration	13
Building Retrofits	18
Pounding Computer Models	20
Earthquake Motions	26
Sample Analysis Results	27
Pounding Study	31
Suggested Pounding Approach	40
Conclusions	40
<u>Appendices</u>	
A: Previous Studies	42
B: Suggested Pounding Approach	44
C: References	48

## **ACKNOWLEDGMENT**

This study was undertaken as the *2010 Special Projects Initiative* of the Structural Engineers Association of Northern California (SEAONC). The funding by SEAONC is gratefully acknowledged. The SEAONC Board contact members were Mark Moore (ZFA Structural Engineers) and Steve Mahin (University of California), and their diligent oversight added greatly to the project. Mark Moore participated in our team meetings and provided timely input as our work progressed. Anindya Dutta (Simpson, Gumpertz & Heger) performed excellent quality assurance by performing parallel verification analyses. The authors are most appreciative of the contributions of many individuals in providing valuable discussions on soft-story buildings including members of the SEAONC Existing Buildings Committee chaired by Marko Schotanus (Rutherford and Chekene) and vice-chaired by Brian McDonald (Exponent Engineers). All opinions and conclusions expressed herein are solely those of the authors.

## INTRODUCTION

Programs to mitigate the hazards of soft-story buildings are gaining momentum in the San Francisco Bay Area as evidenced by recent actions taken by the cities of San Francisco, Berkeley, Oakland and Alameda (*ATC 2009, Department of Elections 2010, Alameda Municipal Code 2010, Berkeley Municipal Code 2010, and Oakland Municipal Code 2010*). In addition, a current project is focusing on solutions to soft-story buildings typically found on the west coast of the United States (*ATC-71-1 2011*).

Many Bay Area soft-story buildings were constructed with their walls close to the property lines, resulting in very little building separation. It is likely such buildings will collide during earthquakes in a phenomenon known as pounding.

Seismic guidelines such as the *International Existing Building Code (IEBC 2009, 2012)* and the seismic rehabilitation standard *ASCE-41 (ASCE 2006)* are not specific about how to account for pounding. *ASCE-41* indicates a separation of four percent of the building height prevents pounding (in lieu of detailed analysis), but waives the requirement for buildings of the same height with matching floor levels. The San Francisco Building Code, recognizing the high density of the city's existing building stock, waives building separation requirements even when seismic upgrade is otherwise triggered (*SFBC 2010*). Other recent soft-story studies are silent about the effects of pounding (*ATC 2009, ATC-71-1 2011*).

Conventional wisdom holds that pounding makes corner buildings more vulnerable and perhaps protects mid-block buildings. This idea is likely based on anecdotal earthquake damage observations and few available computer analysis studies such as Anagnostopoulos (1988), or Athanassiadou et al. (1994). However, prior research mostly considered generic buildings and it is not clear to what degree these apply to the collapse safety of soft-story wood-frame buildings.<sup>5</sup> This was a motivation for our current work, which looks at a particular class of buildings with a specific range of variables representing actual conditions.

This report addresses how pounding affects the collapse performance of certain soft-story wood-frame buildings, with and without retrofit. It provides insight through the computer analysis of actual buildings damaged by the 1989 Loma Prieta earthquake. Various hypothetical pounding situations are analyzed to identify key factors. Using the results, an approximate way to account for the effects of pounding within the context of current design procedures is derived.

---

<sup>5</sup> Several relevant pounding studies are summarized in Appendix A, but none deal specifically with soft-story wood-frame buildings.

## **SAN FRANCISCO SOFT-STORY BUILDINGS**

San Francisco has about 4,400 pre-1973 wood-frame buildings with three or more stories and five or more residential units, considered likely to have soft-story conditions (ATC 2009). Many neighborhoods feature closely spaced buildings filling entire city blocks with corner buildings often larger than their mid-block neighbors (Figures 1a to c). Such buildings can be expected to experience pounding during earthquakes.

A common style of corner building in San Francisco is shown in Figure 1d. It is a four-story wood-frame apartment building of about 12,000 sf constructed in the 1920s. Because of automobile parking on the ground floor level, the first story has relatively few interior walls and the two perimeter street-side walls have numerous garage door openings, making the story flexible and weak relative to those above. We address this type of soft-story building. There are also many relatively newer soft-story buildings with so-called tuck-under parking, often having only one open perimeter wall line, but these are not specifically covered here.

The 1989 Loma Prieta earthquake caused extensive damage in the Marina District. Of 1,452 buildings surveyed in this area (all building types), 63 (4%) were declared unsafe and red-tagged (Harris et al. 1990). A much larger number were damaged and yellow-tagged. Damage was concentrated in 1920s era four-story wood-frame corner apartment buildings and the 81 buildings in this class accounted for six of seven collapses (Figure 2). Many others suffered permanent offsets in the first story, and two that had about 10% story drifts toward the east<sup>6</sup> are shown in Figures 1e and f.

---

<sup>6</sup> The Marina District apparently had greatest intensity shaking in the EW direction as suggested by building damage patterns and Bay Area acceleration records (Hanks and Brady 1991).



(a) Satellite view of city block.



(b) Example of closely spaced buildings.



(c) Example of closely spaced buildings.



(d) Soft-story corner building



(e) Loma Prieta building damage.



(f) Loma Prieta building damage.

**Figure 1.** Examples of San Francisco buildings.

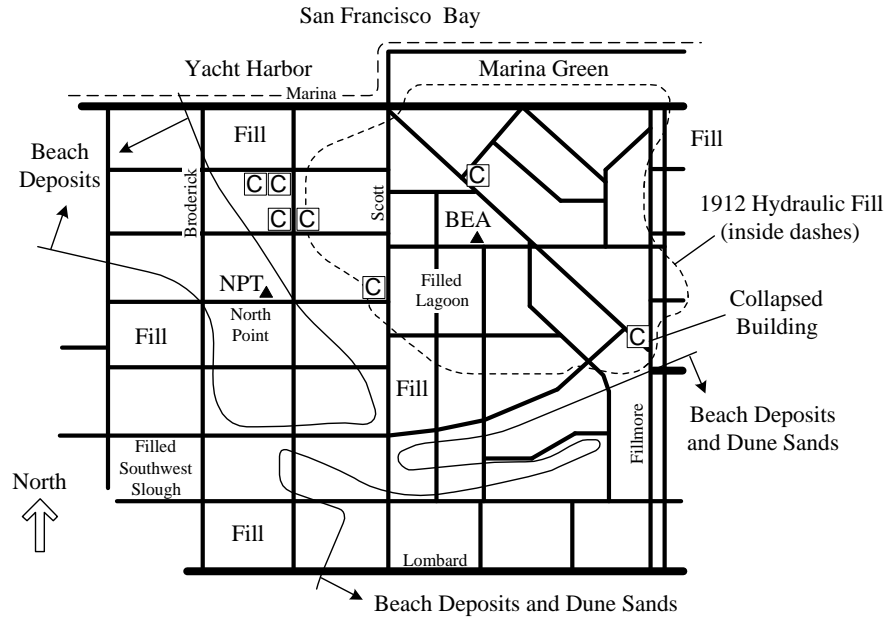


**Figure 2.** Street map of Marina District showing the locations of seven collapsed buildings and soil types. Instruments were located at stations NPT and BEA to record Loma Prieta aftershock motions. USGS estimated main-shock peak accelerations  $\sim 0.25g$  at NPT and  $\sim 0.16g$  at BEA.

### CASE STUDY BUILDINGS

We reviewed the San Francisco Department of Building Inspection (DBI) files to identify candidate Marina District case study buildings that were damaged by Loma Prieta and later retrofitted so that structural drawings showing pre-earthquake wall layout were available. The two buildings selected have the general configuration shown in Figure 3. This style is found throughout the city, and it constituted the majority of the corner buildings in the Marina District (Harris and Egan 1992).

***Building-1.*** This building was selected because it was judged *not* likely affected by pounding, and was close to collapse as evidenced by a reported 10 to 15 degree post-earthquake drift toward the east in the first story (Figure 4). Because there were no nearby adjacent buildings on the east or west sides, it was deemed that pounding did not play a role in the damage and as such, this simplified the calibration process described below. The building wall layouts are shown in Figure 5.

***Building-2.*** This building was also judged *not* likely affected by pounding (Figure 4). It was reported as having slight post-earthquake racking; it was red-tagged, and emergency shoring was installed. On the building's west side, the adjacent building was a two-story house of much lesser mass. A gap of 3 to 4 inches separated the house from the one-story garage portion of the building. The building wall layouts are depicted in Figure 6.



Street-Side Elevation Views

**Figure 3.** Marina District corner building typical geometry. The longitudinal direction is usually oriented in the EW direction.

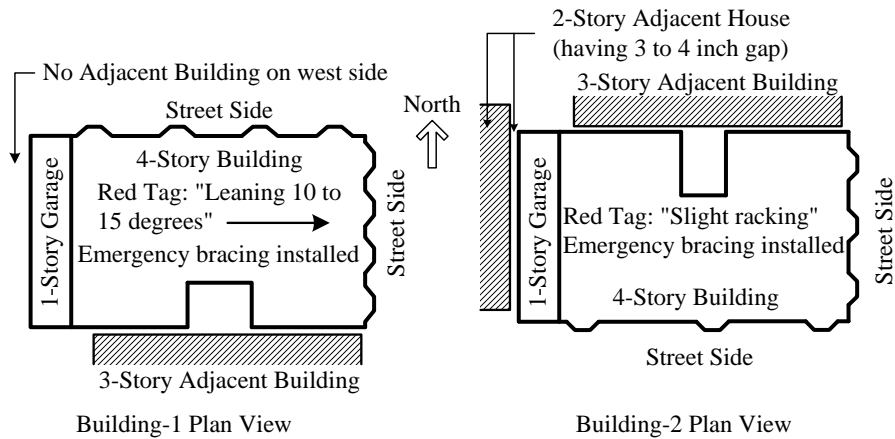


**Figure 4.** Two Marina District case study buildings damaged by Loma Prieta.

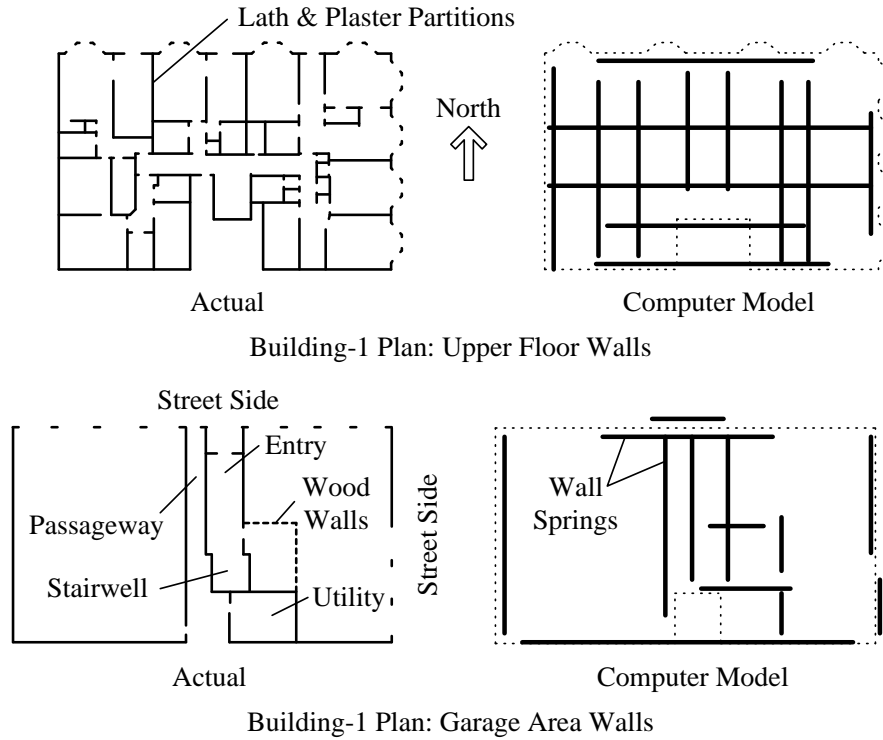


**Figure 5.** Building-1 wall layouts and computer model idealization.

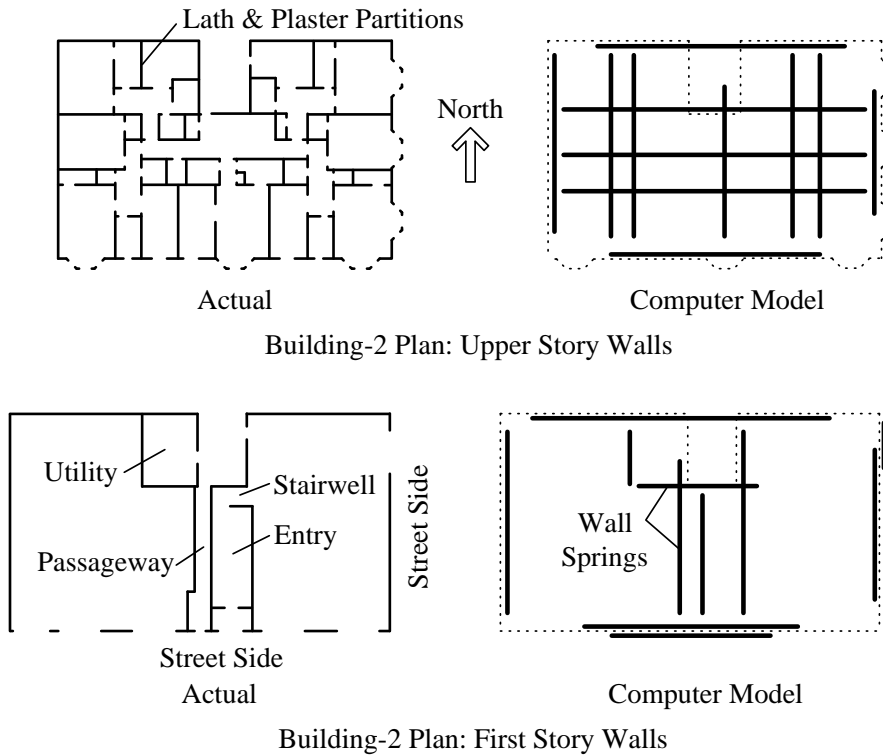


**Figure 6.** Building-2 wall layouts and computer model idealization.

## BUILDING COMPUTER MODELING

Our approach was similar to the SAWS-type computer program formulation developed in the CUREE-Caltech Woodframe Project (Folz and Filiatrault 2001). Buildings were idealized as shear-buildings having rigid floor diaphragms (Figure 7). Walls were modeled as SDOF springs having realistic shear-force versus shear-deformation hysteretic behavior (Figure 8). Table 1 describes the model features. Analysis was carried out using the PC-ANSR computer program (Maison 1992).

**Table 1.** Corner building model features.

Parameter	Description
LFRS	The lateral force resisting system (LFRS) was taken as the walls consisting of non-conforming materials including horizontal boards, stucco, brick veneer, wood lath-and-plaster, and garage doors. Such walls lack hold-downs so gravity loads and cross-walls were assumed sufficient to inhibit substantial uplift. Although not indicated on case study building drawings, buildings of this era sometimes had diagonal wood braces or blocking. When present, the braces typically butted on wooden garage posts (non-ductile compression-only configurations). Due to their brittle nature, such bracing would not be active at large drifts and hence was deemed to have little influence on collapse performance.
Wall spring model	The force-deformation relation (Figure 8) captures key behaviors of the materials in these buildings. These include strength deterioration with increasing deformations, pinching hysteresis with cycling, and reduced unloading stiffness at large deformations. It is a simplified two-parameter version of the empirical model by Kanvinde and Deierlein (2006) for gypsum drywall partitions. Wall lengths in the direction of the springs, excluding door and window openings, were lumped into wall springs using a tributary width approach.
Wall damping model	Wood buildings exhibit considerable damping even under small amplitude vibrations. For small drifts ( $< \sim 0.2\%$ ) as well as cycling on force-deformation unloading branches, the wall model is linear-elastic with no hysteretic action so an additional damping force is provided. The damping model is a frequency-independent type as described by Clough and Penzien (1975) with a limit on the damping force (Figure 9). A value of 5% damping is assigned. This was used instead of the customary viscous damping model because a viscous model is frequency-dependent. The frequencies change significantly when the buildings yield or come in contact during pounding, and the viscous damping forces (damping ratio) thus can change unrealistically.
P-delta spring model	The effects of gravity loads acting on the deflected shape of the building are accounted for as a reduction in the lateral stiffness by the geometric stiffness analogy with a truss bar (Figure 10). P-delta springs are located in each story.
Building mass	Computed equivalent unit floor weights were about 50 psf with wood lath-and-plaster partitions and ceilings contributing about half of the weight.
Additional features	The building models were fixed at the bottom of the ground story for convenience; therefore soil-structure interaction (SSI) was ignored. Inclusion of SSI could add radiation damping, reducing response. It could also result in larger lateral displacements due to rocking and differential settlements, thus causing more pounding. In addition, the ground accelerations were the same at all the buildings; the effects of spatial variation were ignored. Variation in ground motion at each building may lead to increased out-of-phase motions causing more pounding.

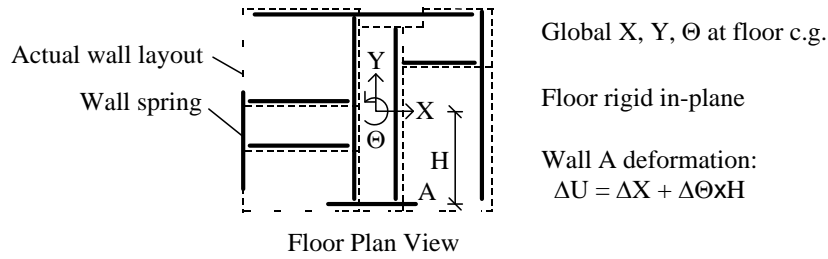


Figure 7. Shear building floor modeling.

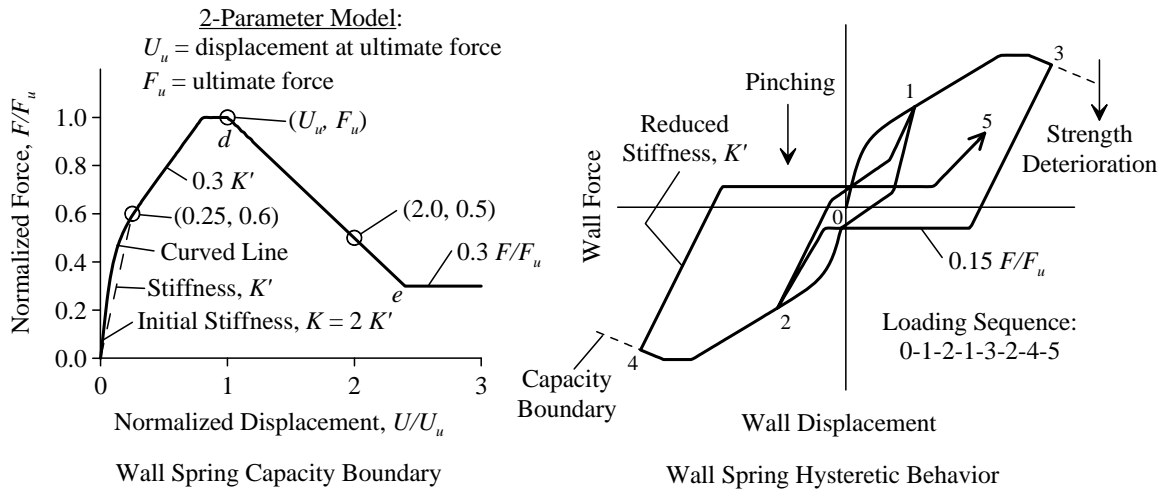


Figure 8. Wall spring model.

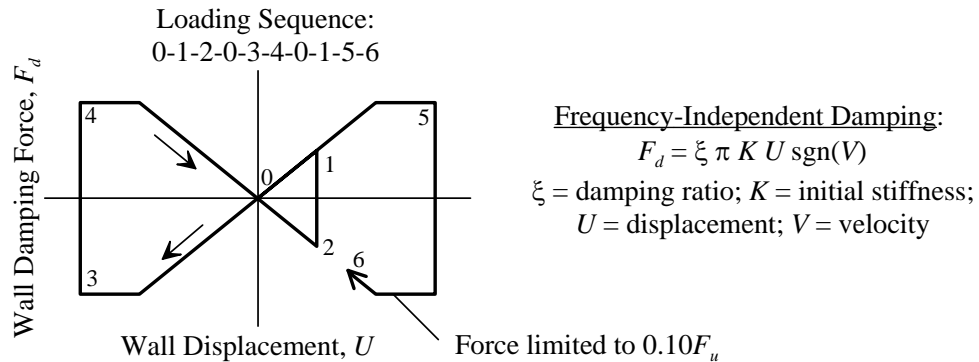
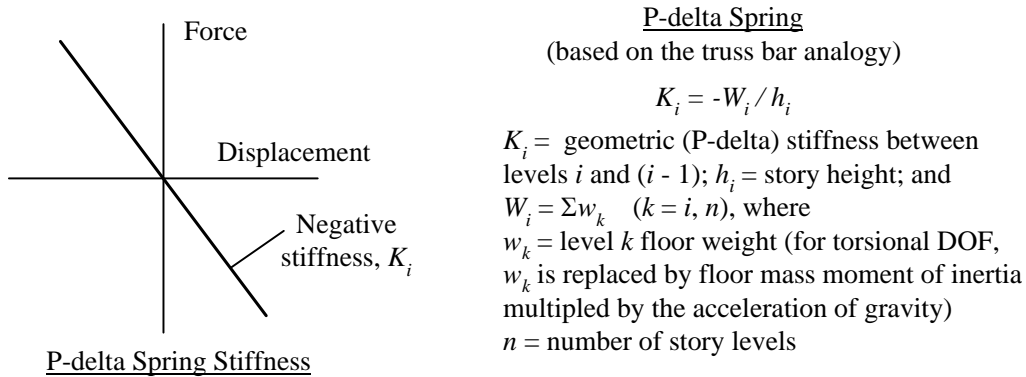


Figure 9. Wall spring damping model.



**Figure 10.** P-delta spring model.

## BUILDING MODEL CALIBRATION

We performed a calibration exercise to estimate the actual strength and ductility of the buildings. Calibrated (i.e., apparent or back-calculated) wall properties were found by tweaking the properties so computer simulations matched the observed near-collapse conditions under Loma Prieta ground motions. Since the first story controlled the behavior, the calibration involved adjusting the first story wall strength and ductility parameters (Figure 8,  $U_u$ ,  $F_u$ , and  $e$ -value).

No recording instruments were in the Marina District at the time of the earthquake, but researchers have estimated the shaking using aftershock data and records from other Bay area soft-soil sites. We took the Treasure Island (TRI) and Outer Harbor Wharf (OHW) records as representative of the shaking, based on studies by Hanks and Brady (1991), and Boatwright et al. (1992). TRI and OHW were recorded about 4 and 7 miles east of the Marina District, respectively, and all three sites had similar epicentral distances of about 60 miles.

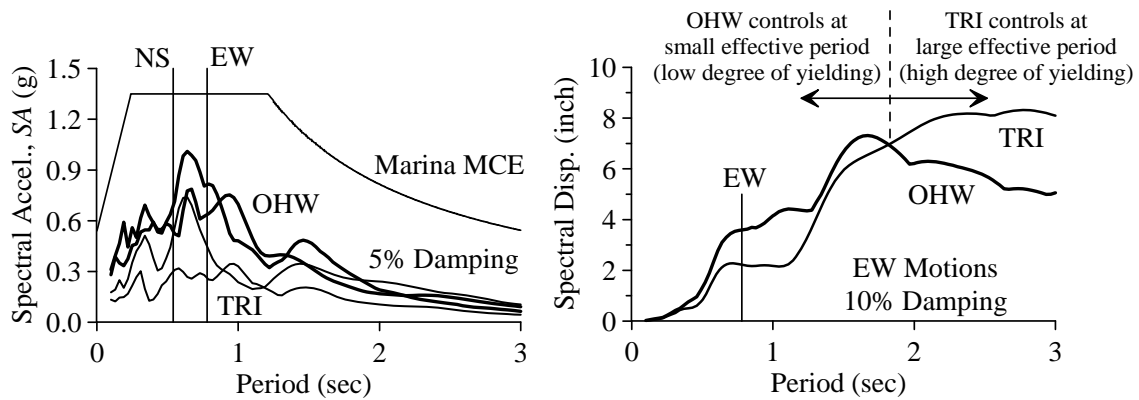
The response spectra are shown in Figure 11. TRI has clear directivity with EW direction spectral values dominating over virtually the entire period range. Because of the uncertainty as to which records best depict the actual shaking at the specific building sites, our calibration criterion was that the building models must be able to just survive *either* the TRI or OHW motions. This was determined via incremental dynamic analysis (IDA).

Figure 12 illustrates the IDA process using the response from the OHW records scaled to different intensities. The displacement patterns are similar until a point of instability occurs and the building collapses when the earthquake is scaled by a factor of  $I = 1.3$ . (See the Pounding Study section for a description of the collapse criteria.)

IDA curves from models having wall properties that led to a reasonable match with Loma Prieta are presented in Figure 13. At the Loma Prieta intensity ( $I = 1.0$ ), the TRI records produced peak story drifts of about 5% toward the east in both buildings. Building-1 collapsed for  $I > 1.0$ . For intensities below about  $I = 0.8$ , the OHW records produced

greater drifts. This could be expected, since the OHW spectral values were higher at the buildings' fundamental periods (Figure 11). The pattern was reversed for larger intensities with the TRI records producing greater drifts. Apparently as the first story softened and lengthened the periods, the TRI spectral displacements in the long period range (> 2 sec) dominated (Figure 11). This indicates the important role long period ground motions played in the buildings' performance.

The first floor wall layouts of the buildings somewhat differ (Figures 5 and 6), but the story strengths and small amplitude natural periods were within about 10% of each other. Both buildings were weakest in their EW directions, with strengths equal to about 13% of the building weight. The effective modal masses indicated the modes were virtually uncoupled in each principal direction, implying that torsion irregularity was not as severe as might be thought from inspection of the first story wall layouts.



**Figure 11.** Acceleration and displacement response spectra for Treasure Island (TRI) and Outer Harbor Wharf (OHW) records (two components each). Building fundamental periods denoted by vertical lines.

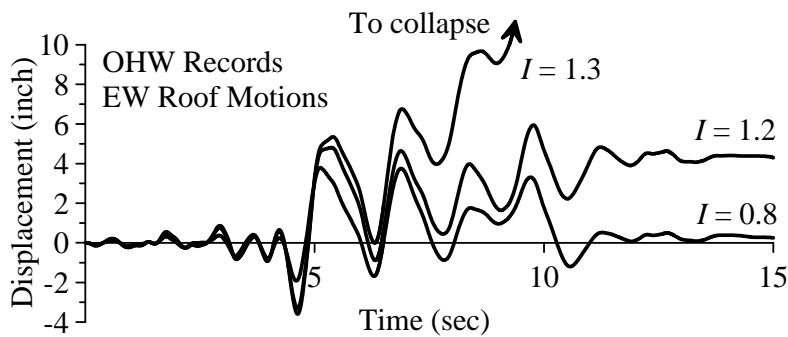


**Figure 12.** Building-1 response under different earthquake intensities.

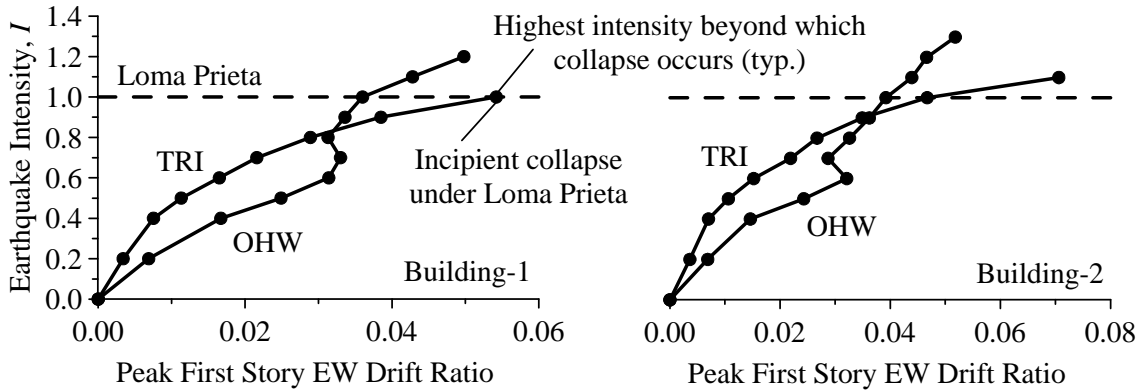


**Figure 13.** Incremental dynamic analysis (IDA) curves for Building-1 and Building-2 using calibrated wall properties. The TRI and OHW spectra cross over each other (Figure 11), and this is probably why the IDA curves cross.

### Calibrated Wall Properties

Table 2 contains the calibrated wall properties for the nine wall types used in the computer models. We used our judgment in assigning the strength and ductility parameters *relative* to each other using test data (Thayer 1956) and *ASCE-41* as guidance. The calibrated properties collectively simulated first story performance from Loma Prieta. For the upper stories, the parameters were set consistent with the first story values using our judgment.

**Table 2.** Calibrated and ASCE-41 wall properties.

First Story			
Type	$U_u^1$	$F_u^2$	Assumed Construction <sup>3</sup>
1. Perimeter walls facing street	0.025 [0.0073]	1,000 [350]	Stucco or brick veneer over horizontal boards on the outside; sheet metal (fire protection) and perhaps horizontal boards on the inside. Wall studs may have diagonal blocking in places. [stucco] <sup>4</sup>
2. Perimeter walls facing adjacent buildings	0.035 [0.017]	500 [80]	Horizontal boards on the outside; sheet metal and perhaps horizontal boards on the inside. Wall studs may have diagonal blocking in places. [horizontal boards]
3. Stairwell, entry way, passageway	0.015 [0.019]	600 [400]	Wood lath-and-plaster on one side and sheet metal on the other. [wood lath-and-plaster]
4. Utility room	0.015 [0.019]	600 [400]	Hollow clay tile wall. [wood lath-and-plaster]
5. Wood partitions	0.035 [0.017]	400 [80]	Horizontal boards on one or both sides. [horizontal boards]
6. Garage door	0.05 [0]	1,500 [0]	Based on tests of wood panel type (Kornfield and Buscovich 2009). $F_u$ = force per door. [none]
Upper Stories			
7. Perimeter walls facing street	0.025 [0.019]	1,400 [400]	Stucco over horizontal boards on the outside; wood lath-and-plaster on the inside. Wall studs may have diagonal blocking in places. [wood lath-and-plaster]
8. Perimeter walls facing adjacent buildings	0.025 [0.019]	800 [400]	Horizontal boards on the outside; wood lath-and-plaster on the inside. Wall studs may have diagonal blocking in places. [wood lath-and-plaster]
9. Interior partitions	0.015 [0.019]	1,200 [800]	Wood lath-and-plaster on both sides. [wood lath-and-plaster]
<sup>1</sup> $U_u$ = story drift ratio at onset of strength deterioration. <sup>2</sup> $F_u$ = peak unit force (pounds per linear foot of wall). For garage doors, $F_u$ is the peak force per door. <sup>3</sup> Assumed construction because retrofit drawings indicated pre-Loma Prieta wall layouts but not exact wall compositions. <sup>4</sup> Values in brackets are ASCE-41 default strength (from ASCE-41 Table 8-1) and ductility (Equation 8-1 and Table 8-3). Only one material type from each assembly was considered because ASCE-41 ignores the weaker sheathing materials in composite walls (Section 8.4.1).			

### Calibrated vs. ASCE-41 Properties

For our study buildings, using *ASCE-41* for material property selection—as might be done in practice—led to unrealistically weak and brittle models. Figure 14 illustrates this by comparison of IDA curves using the TRI records for Building-1. The model based on *ASCE-41* had incipient collapse at only 27% of the Loma Prieta intensity with a peak drift ratio of 0.024. The calibrated model has much greater strength and ductility, implying that *ASCE-41* properties can be overly conservative.

We think there are several reasons for this discrepancy. First, there is a paucity of lab test data on archaic wall materials, so *ASCE-41* values were probably set understandably low to be safely conservative. *FEMA-273/274* (*ASCE-41*'s predecessor) pointed out the lack of data and admitted that many of its archaic material properties were “estimates” (*FEMA-273/274* 1997). *ASCE-41* properties are virtually the same as those in *FEMA-273*.

Second, the calibrated properties reflect entire first story wall assemblies including cross-wall flange action and out-of-plane bending, whereas *ASCE-41* considers only wall in-plane behaviors and ignores the weaker sheathing materials in composite walls.

Finally, *FEMA P440A* (2009) found that in most cases, in-cycle strength degradation controls nonlinear dynamic behavior (the *d* to *e* segment in Figure 8), and that a backbone curve derived from an envelope of lab cyclic test data can be overly conservative. In many cases, backbone curves derived from monotonic test data were found to be better models. *ASCE-41* material properties represent cyclic envelopes, and this is another source of conservatism.

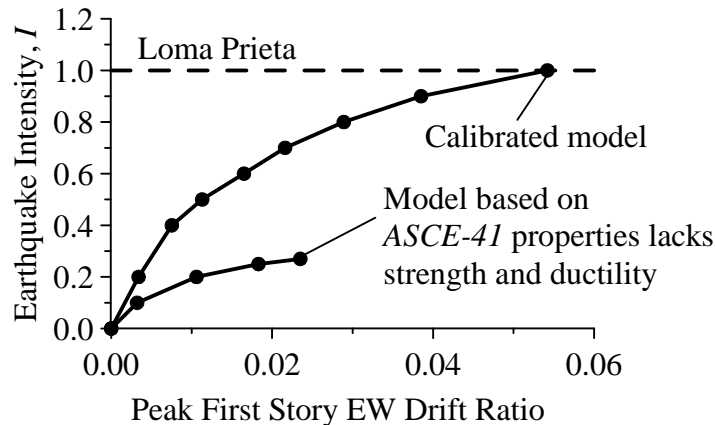


**Figure 14.** Comparison of IDA curves for Building-1 using calibrated model (Table 2 properties) and model based on *ASCE-41* (Table 2 values in brackets). Calibrated model collapses for  $I > 1.0$ , and *ASCE-41* model collapses for  $I > 0.27$ .

## BUILDING RETROFITS

We created hypothetical retrofits based on Chapter A4 of the *International Existing Building Code (IEBC 2012)*, titled “Earthquake Risk Reduction in Wood-Frame Residential Buildings with Soft, Weak or Open-Front Walls.” Chapter A4 is available for use by any California jurisdiction, and San Francisco accepts its use for voluntary retrofit.

Chapter A4 is a prescriptive procedure for retrofitting the ground story of soft-story buildings. It is based on earthquake design provisions for new construction, but requires only 75 percent of the design base shear and exempts the upper stories from any work. For computing the base shear, the *IEBC* uses a response modification coefficient  $R$  (the smaller the  $R$ -value, the larger the design force). The *IEBC 2009* and earlier editions restrict the  $R$ -value to that of the existing walls above. For nonconforming archaic materials like those in the case study buildings, the resulting  $R$ -value is very small. This leads to very strong and stiff retrofit systems thought to be both unnecessary and, in some cases, capable of forcing failure into the upper stories. The *IEBC 2012* edition, which we used, relaxes this restriction as long as the retrofit strength and stiffness is sufficient to eliminate the defined soft- and weak-story irregularities.

We considered retrofits according to the 2012 *IEBC* for three sites in San Francisco (Pacific Heights, Richmond District, and Marina District), then created two generic retrofits of Building-1.

- Retrofit-A represents a first story upgrade with first story strength equal to about 65% of the second story strength. This remedies an *extreme weak story* irregularity (defined as a ratio of first story to second story strength less than 65 percent).
- Retrofit-B represents a retrofit with about 85% of the second story strength and remedies a *weak story* irregularity (defined as a ratio less than 80 percent).

Story strength ratios for the as-built and retrofitted buildings are shown in Table 3. Note that the required retrofit strengths were based on the building *calibrated* strength, which was larger than *ASCE-41* would have prescribed (Figure 14). Therefore, our retrofitted buildings might be stronger than those based on an *ASCE-41* design.

We assumed retrofits consisting of wood materials (lumber and plywood) having hysteretic behavior as shown in Figure 8. Computer models of the retrofitted buildings were created by adding wall springs having the required strengths,  $F_u$ , at a peak force drift ratio,  $U_u$ , of 0.025.

Retrofits using other materials could have strength degradation point ( $U_u$ ) and hysteretic behavior different from what we assumed, and this might change the analysis results. For a steel moment frame retrofit, we would expect better performance since a steel frame would have more ductility and robust hysteretic action than the wood retrofit we assumed.

Static pushover curves illustrating the story stiffness, strength, and ductility are shown in Figure 15. The static collapse drift (SCD) ratio is the drift beyond which the building collapses under gravity loads, and represents a theoretical upper bound capacity. A building’s permanent drift must be less than the SCD in order to remain standing. For the as-built Building-1, the SCD ratio was 0.087. Considering that Building-1 was reported as leaning 10 to 15 degrees after Loma Prieta (drift ratio > 0.1), the calibrated properties might still be conservative. Retrofit-A had a SCD ratio of 0.12, indicating the ability to sustain greater drifts and yet remain standing.

**Table 3.** As-built and retrofitted Building-1 story strength ratios and periods.

Structure	EW Strength (Force/Weight <sup>1</sup> )	NS Strength (Force/Weight)	T <sub>EW</sub> <sup>2</sup> (sec)	T <sub>NS</sub> <sup>2</sup> (sec)	T <sub>TOR</sub> <sup>2</sup> (sec)
As-built first story	0.13	0.22	0.80	0.53	0.53
As-built second story	0.50	0.55	--	--	--
<i>IEBC</i> first story <sup>3</sup>	0.33 to 0.40	0.34 to 0.40	0.32	0.32	--
Retrofit-A first story <sup>4</sup>	0.33	0.37	0.53	0.46	0.43
Retrofit-B first story <sup>5</sup>	0.43	0.47	0.48	0.43	0.40

<sup>1</sup> Weight refers to total building weight.  
<sup>2</sup> T<sub>EW</sub>, T<sub>NS</sub>, T<sub>TOR</sub> refer to building periods in EW, NS, and torsion directions. For the *IEBC* retrofit, the period shown is from the *ASCE 7-05* default period formula. Elastic fundamental periods estimated assuming a first story mechanism were 0.52 sec (EW) and 0.37 sec (NS).  
<sup>3</sup> *IEBC* indicates required first story strengths per Chapter A4 of the 2012 *IEBC* and *ASCE 7-05*. The range results from particular location and soil type in San Francisco. Strength ratios as follows (remedy of weak-story irregularity did not always control):  
 Pacific Heights: 0.33 (EW) and 0.37 (NS).  
 Richmond District: 0.40 (EW) and 0.40 (NS).  
 Marina District: 0.33 (EW) and 0.34 (NS).  
<sup>4</sup> Retrofit-A upgrades the first story to about 65% of the second story strength.  
<sup>5</sup> Retrofit-B upgrades the first story to about 85% of the second story strength.

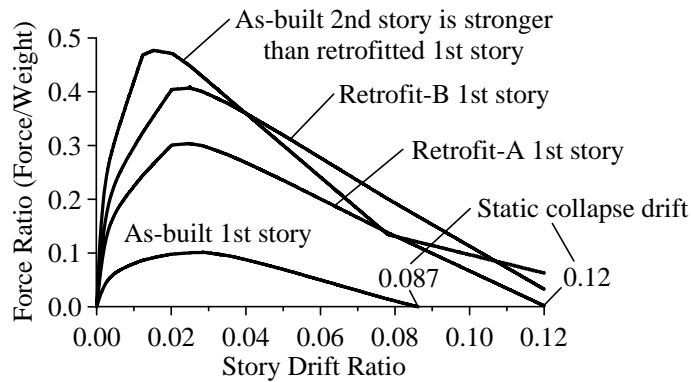


**Figure 15.** EW direction static story pushover curves for as-built and retrofitted buildings (includes P-delta effects). Note how retrofits add both strength and ductility.

## POUNDING COMPUTER MODELS

The case study was a building located on a street corner having the same general configuration as the corner buildings described above. The offset from the one-story attached garage portion, common in many buildings but not always present, was ignored so that pounding could occur at any of the stories along two sides of the building. Our study focused on the collapse performance of the corner building.

In San Francisco, mid-block buildings are often of the same age and construction as corner buildings, but the corner buildings typically have more stories and larger footprints. Our pounding model had a corner building with four three-story adjacent mid-block buildings on each of two perpendicular sides (Figures 16 and 17).

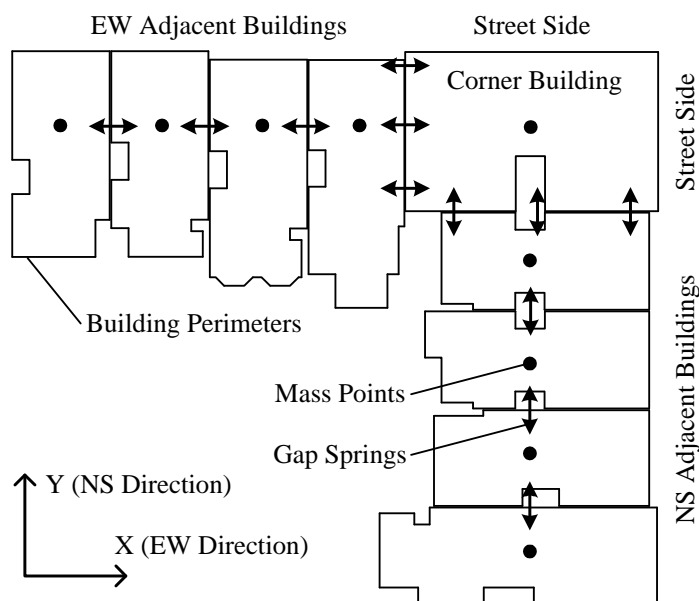


**Figure 16.** Pounding model plan view.

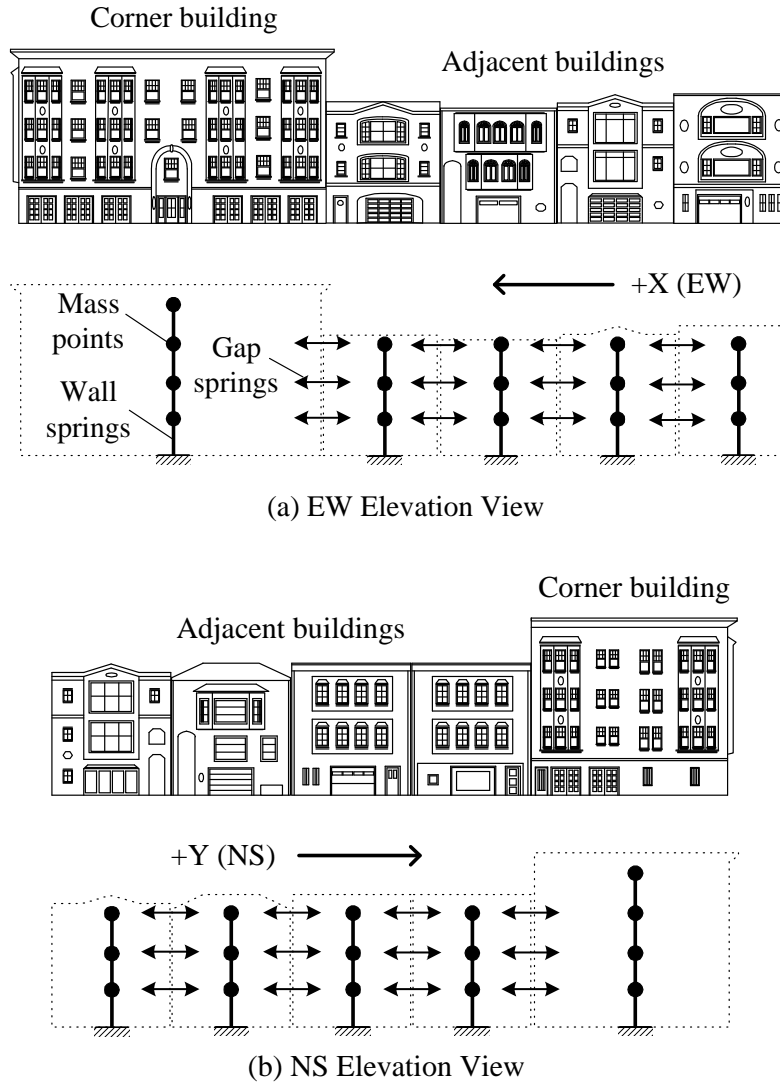


**Figure 17.** Pounding model elevation views.

***Base-Case Pounding Model***

We formulated a *base-case* pounding situation to depict a condition reasonably typical of San Francisco corner buildings. The calibrated Building-1 model described above was used as the corner building. We assumed adjacent mid-block buildings of wood construction, each weighing one-half that of the corner building, with one-inch effective separations (gaps) between all buildings.

We believe our *base-case* model is complete enough to capture the important actual field conditions, though it does involve simplifying assumptions needed to keep the analysis manageable. Table 4 describes the *base-case* in detail. Two notable assumptions follow.

Linear-elastic adjacent buildings. The adjacent mid-block buildings were modeled with direct-displacement design concepts that idealize a wood building as linear-elastic, with an effective period and damping (Filiatrault, et al. 2003). The effective period (~0.94 sec) was set longer than the small amplitude linear-elastic value to account for inelastic softening (like a secant stiffness effect). The effective damping (20%) was set larger than the customary 5% value to account for inelastic hysteretic energy dissipation.

This simplifying assumption was made in order to focus on the corner building that is modeled as nonlinear and can collapse. While we believe this is appropriate to the nature of our study, it means that the adjacent buildings, modeled as elastic, cannot collapse. In particular, they cannot collapse like toppling dominos onto the corner building, and the corner building cannot collapse in the direction of the adjacent buildings. In our model, corner building collapse under pounding can only occur toward the street. The effects from explicit nonlinear models of the adjacent buildings, studied here in only two cases, could be a topic for separate studies.

One inch effective gap distances between all buildings. Some post-Loma Prieta retrofit drawings indicate perimeter walls were located one inch from property lines, but we do not know how accurate or universal this practice was. Our San Francisco street-side field inspections found it often difficult to confirm building separations due to veneers, flashings or filler boards between the buildings. Hence, there are often zero gaps at the street-side building corners. Where the gaps were exposed, we noted separations on the order of two to three inches at ends of buildings near the street. However, light passing through the gaps was often sporadic indicating some blockage perhaps from debris and/or bowing walls. It was common to observe buildings slightly out-of-plumb so the gap size varied over the height. We deemed the one-inch effective gap as the most reasonable uniform condition for the *base-case* model.

**Table 4.** The *base-case* pounding conditions.

Parameter	Description
Adjacent bldg. modeling	Planar linear-elastic models. See text for discussion.
Number of adjacent bldgs.	Four adjacent buildings located on two sides of corner building were judged to be the maximum number that could interact with the corner building.
Height of adjacent bldgs.	Adjacent buildings were assumed to be three stories in height. In San Francisco, corner buildings typically have more stories than mid-block buildings
Adjacent building stiffness	Because the front portions of mid-block buildings typically have relatively open parking and storage areas at the first floor, the first story was assigned one-third the stiffness of the upper stories.
Adjacent building mass	Adjacent buildings each have one-half the total mass of corner building. This assumption was based on our study of satellite images of typical building footprint areas and numbers of stories.
Adjacent building periods	The effective period was set at ~0.94 sec based on wood building direct-displacement design concepts. Periods were varied by $\pm 10\%$ so that buildings will not vibrate completely in-phase (period pattern: 0.94, 1.03, 0.94, 0.85 sec).
Adjacent bldg. damping	Effective damping of 20% was used based on wood building direct-displacement design concepts. Frequency-independent type assigned.
Pounding locations	Buildings were assumed to impact at common floor elevations. In reality, floors do not always align in elevation, so impacts between floor levels are possible. However, interior cross-walls (typically stiff and strong lath-and-plaster) act as stiffeners to distribute the collision forces to the floors above and below. Hence, for these buildings, impacts between floors may be expected to have stiffness similar to floor-level impacts.
Buildings gaps	Modeled as 1 inch. See text for discussion.
Contact spring stiffness	Linear-elastic springs having total stiffness of 400 k/in at each floor level were used (Figure 18). Stiffness was chosen so that peak spring deformations were on the order of one inch because we deemed this a realistic amount of local flexibility. For buildings immediately adjacent to the corner building, three springs were used having 100 k/in at floor corners and 200 k/in at floor mid-length. The pounding analysis results were not sensitive to contact spring stiffness when varied around these values (the contact spring force did vary but the global building behavior was not appreciably changed).
Contact spring damping	Spring damping was set at 22% based on a coefficient of restitution of 0.5 per test data (Jankowski 2009) and consideration of local vibration mode energy absorption effects (Nathan 2000). Frequency-independent type assigned.

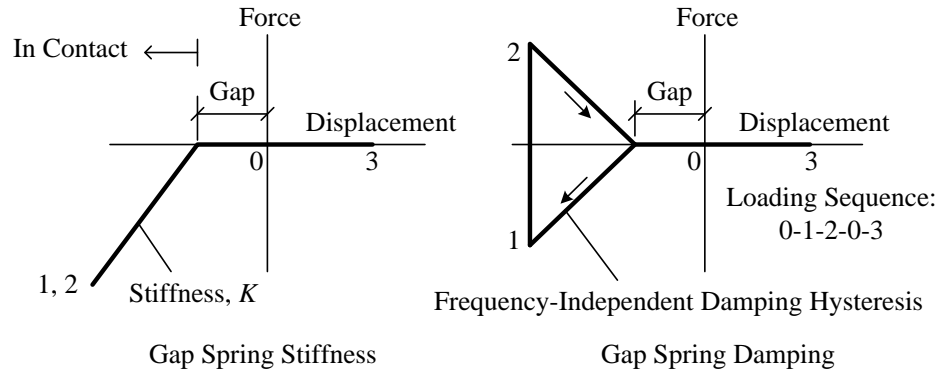


**Figure 18.** Gap spring model.

### Additional Pounding Cases

We formulated twenty-one different pounding cases in addition to the *no-pounding* and *base-case*. The corner building model was the same for all cases. The additional cases had variations in the adjacent building properties to assess the influence of various factors on the collapse performance of the corner building. Key parameters that were varied include building separation (gap) distances and adjacent building energy dissipation (effective damping), effective period (stiffness), and mass. Table 5 describes the cases we studied.

**Table 5.** Cases studied.

Case	Description
a. <i>No-pounding</i>	Model as described previously, with no adjacent buildings.
b. <i>Base-case</i>	Described in Table 4.
c. <i>Single-building</i>	Only one adjacent building included on each side. Many actual situations have variable gap sizes within the series of adjacent buildings, so this represents a lower bound pounding case.
d. <i>Stiff-case</i>	Adjacent buildings with periods of ~0.38 sec. This is the period for concrete moment frames per <i>ASCE-41</i> . Intended to represent adjacent buildings of different type. Effective stiffness is about 7 times that of <i>base-case</i> .
e. <i>Rigid-case</i>	All adjacent buildings completely rigid. This was intended to approximate very stiff adjacent buildings such as concrete shear wall structures.
f. <i>Severe-case</i>	Adjacent buildings each having: 10% damping, zero gaps, and mass 2 times that of corner building. This was expected to represent a hazardous upper bound. Adjacent buildings stiffness adjusted to have periods ~0.94 sec.
Cases to examine effect of gap size	
g. <i>Base w/ 0 inch</i>	<i>Base-case</i> with effective building separations of 0 inches for all buildings.
h. <i>Base w/ 2 inch</i>	<i>Base-case</i> with effective building separations of 2 inches for all buildings.
i. <i>Base w/ 4 inch</i>	<i>Base-case</i> with effective building separations of 4 inches for all buildings.
j. <i>Severe w/ 1 inch</i>	<i>Severe-case</i> with effective building separations of 1 inch for all buildings.
k. <i>Severe w/ 2 inch</i>	<i>Severe-case</i> with effective building separations of 2 inches for all buildings.
l. <i>Severe w/ 4 inch</i>	<i>Severe-case</i> with effective building separations of 4 inches for all buildings.
Cases to examine the effect of adjacent building damping	
m. <i>Base w/ 5%</i>	<i>Base-case</i> with adjacent buildings having 5% effective damping.
n. <i>Base w/ 10%</i>	<i>Base-case</i> with adjacent buildings having 10% effective damping.
o. <i>Stiff w/ 5%</i>	<i>Stiff-case</i> with adjacent buildings having 5% effective damping.
p. <i>Stiff w/ 10%</i>	<i>Stiff-case</i> with adjacent buildings having 10% effective damping.
Cases to examine the effect of adjacent building mass	
q. <i>Base w/ 1.0 mass</i>	<i>Base-case</i> with each adjacent building having mass equal to that of corner building. Stiffness adjusted to maintain adjacent building periods ~0.94 sec.
r. <i>Base w/ 2.0 mass</i>	<i>Base-case</i> with each adjacent building having mass 2 times that of corner building. Stiffness adjusted to maintain adjacent building periods ~0.94 sec.
s. <i>Severe w/ 0.5 mass</i>	<i>Severe-case</i> with each adjacent building having mass one-half that of corner building. Stiffness adjusted to maintain adjacent building periods ~0.94 sec.
t. <i>Severe w/ 1.0 mass</i>	<i>Severe-case</i> with each adjacent building having mass equal to that of corner building. Stiffness adjusted to maintain adjacent building periods ~0.94 sec.
Cases to examine effect of modeling features	
u. <i>Sign-flip</i>	<i>Base-case</i> with sign change on earthquake inputs (plus to minus) to examine effects of randomness within the motions that make up the suite of earthquakes. This case can also be understood to represent an identical <i>base-case</i> building on the diagonally opposite street corner.
v. <i>NL-next-door</i>	Same as <i>base-case</i> except buildings immediately adjacent to corner building assigned nonlinear behavior (those beyond are linear-elastic). Instead of having a constant effective period and damping, the nonlinear buildings automatically make adjustments via hysteretic actions during the earthquake. Model formulation is like that for the corner building having idealized wood building behaviors. Upper story strength of 0.4 times the weight of the building, and first story strength of 0.2 times the weight of the building.
w. <i>NL-zero-gaps</i>	Same as <i>NL-next-door</i> but with zero separations between all buildings.

## EARTHQUAKE MOTIONS

We used the far-field record set from *FEMA P695* (2009), also known as the *ATC-63* suite. This suite was chosen for practicality, as it represents a benchmark having a logical basis, and its use here facilitates comparison with other studies using the same suite. It contains twenty-two pairs of earthquake records intended to represent shaking from strong earthquakes ( $M > 6.5$ ) at soil sites located greater than 10 km from source. There is considerable variability across the suite as indicated by a coefficient of variation (COV) of 42% in the short period range (Figure 19).

When the suite is scaled to a median spectral acceleration of 1.0g at 0.3 sec period, the mean spectrum matches two-thirds of the Maximum Considered Earthquake for a rock site ( $MCE_{rock}$ ) in the Pacific Heights District of San Francisco per *ASCE 7-05* (2005). We denote this as a Design Earthquake on rock ( $DE_{rock}$ ). The mean spectrum for periods greater than 0.5 sec lies well below the spectra for the Richmond and Marina District sites, indicating the suite is *not* consistent with the *ASCE 7-05* seismic hazards for those stiff- and soft-soil sites (Figure 19). However, the mean spectrum is comparable to the spectra from the TRI and OHW records used previously to represent shaking in the Marina District during Loma Prieta (Figure 11).

Also note that the suite lacks the ground motion pulse effects that can occur at sites close to active faults (near-field), so the influence of near-field earthquakes on our results is unknown. *FEMA P695* indicates that near-field motions reduce collapse safety margins (relative to far-field motions); hence our results might understate the collapse risk in certain situations.

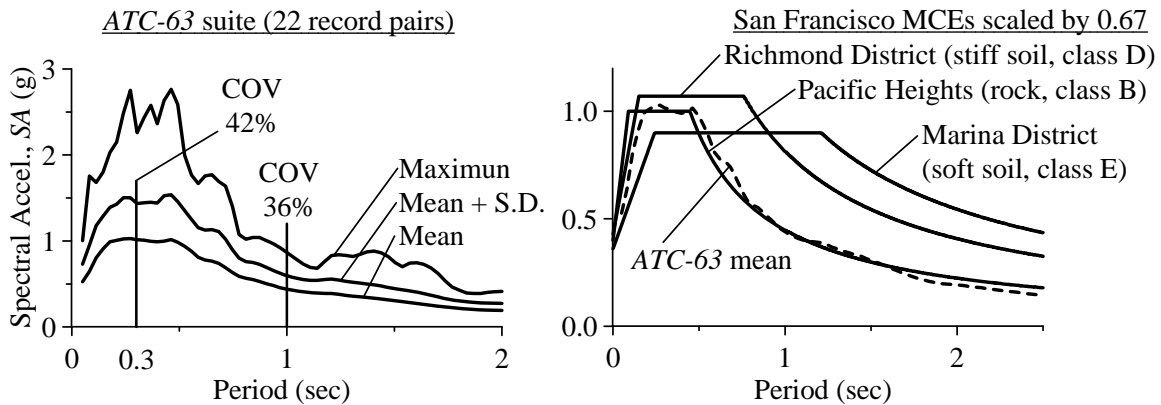


**Figure 19.** Response spectra statistics of *ATC-63* suite (5% damping) and comparison to *ASCE 7-05* Design Earthquakes (0.67xMCE) for sites in San Francisco.

## SAMPLE ANALYSIS RESULTS

The following are sample results that illustrate response behaviors.

Hysteretic actions with no pounding. Much of the response of the as-built structure was on yield plateau segments having very low strength and stiffness (Figure 20). In essence, once the first story suffered damage, the building above swayed back and forth in a precarious manner. In contrast, the retrofitted building had greater strength and ductility, so its response was more stable.

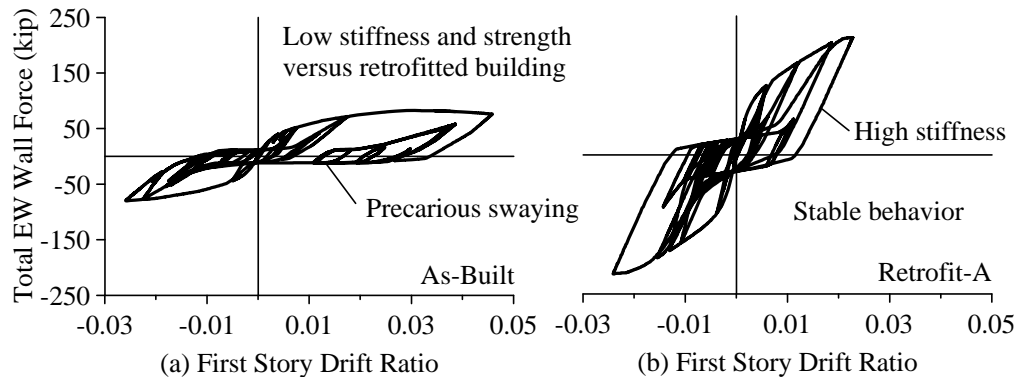


**Figure 20.** Sample first story EW hysteretic response from the same earthquake.

Pounding time histories. Figure 21 shows as-built and Retrofit-A *base-case* building time history motions from different earthquakes in which the corner building did not collapse. These do not necessarily represent the most common response patterns since there was considerable variability in the motions due to the wide variance in the ATC-63 suite, but they help explain aspects of pounding response.

Because the corner and adjacent buildings were of wood-frame construction and similar heights, they can be expected to have similar inelastic actions translating to similar high effective damping and long effective periods. This causes strong in-phase motions as explained in detail by Jeng et al. (1992). The result was few impacts until the corner building experienced sufficient yielding so its motions became out-of-phase with the adjacent buildings. With the as-built corner building, all the buildings moved in close unison before the first collision occurred. The adjacent buildings rapidly returned to in-phase motions after collisions because their dynamic properties were all nearly the same. Similar behavior was shown in Retrofit-A. After the corner building experienced a certain amount of yielding, it started to move out-of-phase, collided, and then was forced briefly into synchronous motion with the adjacent buildings, with this sequence repeating during the earthquake.

A series of buildings should have more pounding as their dynamic properties become more varied leading to out-of-phase motions. Dynamic property variation may come from aspects such as differing structural systems (stiffness), building heights (periods), or

yielding behaviors (strength or hysteretic action). Other factors that ought to increase interaction include lower effective damping (causing larger displacements and higher likelihood for out-of-phase motions) and smaller building separations (increasing the likelihood of contact). These factors are consistent with findings by others (Appendix A contains a summary).

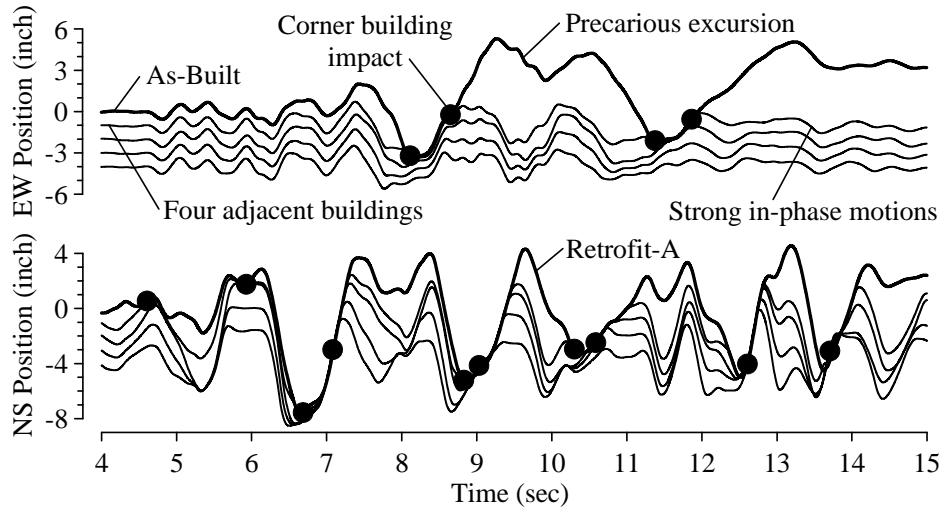


**Figure 21.** Sample *base-case* as-built and Retrofit-A pounding time history motions from different earthquakes. Motions are for 4<sup>th</sup> floor of corner building and roof levels of adjacent buildings. Solid dots denote impacts at the corner building central spring. Impacts at the corner building outside springs and impacts between adjacent buildings are not shown.

Contact stiffness and impact force. The collisions generated large forces acting over brief contact durations (Figure 22). The buildings generally did not lean and grind on each other for long durations. We performed several analyses with different contact spring stiffness values and found it had an effect on the peak impact force but relatively small influence on the building global collapse behavior, at least for the stiffness range considered.

Possible local damage caused by impact forces was not considered in our study. Because the buildings have flat sides with no hard protrusions, we deemed that concentrated damage, such as buckling of walls or punching of holes from pounding, were not sufficiently generic as to be of practical concern in our study on building collapse.

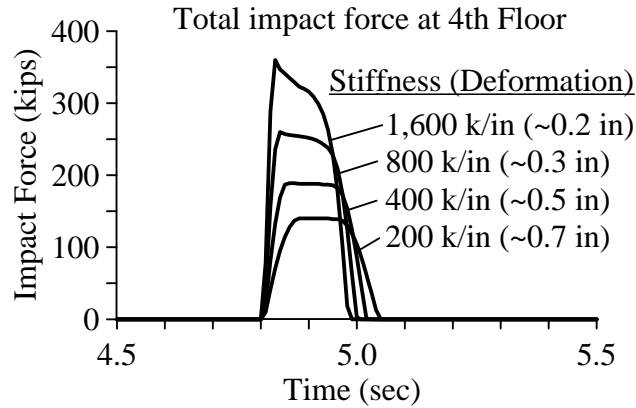


**Figure 22.** Sample impacts with different contact spring stiffness for the case of pounding with rigid adjacent building (*rigid-case*).

Collapse variability within ATC-63 suite. Directions of collapse for *no-pounding* and *base-case* pounding for the twenty-two earthquakes are given in Table 6. For the pounding model, adjacent buildings prevent collapse in the negative direction. For  $DE_{rock}$  shaking, the as-built *no-pounding* had 10 collapses (4 positive and 6 negative) and *base-case* pounding had 12 collapses. Pounding simply turned 5 of the 6 *no-pounding* negative collapses into positive collapses, saved one collapse (EQ6) and generated 3 others (EQ16, 17, 18). (See the Pounding Study section for a description of the collapse criteria.)

For  $MCE_{rock}$  shaking, the retrofitted building *no-pounding* had 10 collapses (4 positive and 6 negative) and *base-case* pounding had 9 collapses. Pounding turned 5 of the 6 *no-pounding* negative collapses into positive collapses and saved one collapse (EQ4), but it generated no additional collapses.

Our study measured collapse performance in the aggregate—the number of collapses in a suite of earthquakes. We did not quantify the detailed change in outcomes for each record as in Table 6, for the numerous pounding analyses. Therefore, if a pounding case results in the same number of collapses as the *no-pounding* case, but the records that led to collapse were different, we still count that as a nil effect of pounding. This is the conventional practice for measuring fragility. However, the phenomenon by which pounding changes the criticality of certain records while resulting in the same aggregate collapse rate, and what that might say about the accuracy of a conventional *no-pounding* model when pounding is possible, is probably worth separate study.

**Table 6.** Direction of collapse according to the specific earthquake in the *ATC-63* suite.

Earthquake	As-built $DE_{rock} (SA^1 = 1.0g)$		Retrofit-A $MCE_{rock} (SA = 1.7g)$	
	No-pounding <sup>2</sup>	Pounding <sup>3</sup>	No-pounding	Pounding
EQ1	P <sup>4</sup>	P	P	P
EQ2	<sup>5</sup>		N	P
EQ3	N <sup>6</sup>	P	N	P
EQ4	N	P	N	
EQ5	N	P	N	P
EQ6	N			
EQ7				
EQ8	P	P		
EQ9				
EQ10				
EQ11	P	P	P	P
EQ12	P	P	P	P
EQ13	N	P	N	P
EQ14				
EQ15				
EQ16		P		
EQ17		P		
EQ18		P	P	P
EQ19				
EQ20				
EQ21	N	P	N	P
EQ22				

<sup>1</sup> SA = median spectral acceleration at 0.3 second period of scaled *ATC-63* suite.  
<sup>2</sup> No-pounding results are from *no-pounding* case.  
<sup>3</sup> Pounding results are from *base-case*.  
<sup>4</sup> P means collapse in positive direction (+X or +Y).  
<sup>5</sup> Blank field means the building did not collapse.  
<sup>6</sup> N means collapse in negative direction.

## POUNDING STUDY

We analyzed the as-built and retrofitted building models to assess the influence of pounding on the *collapse performance* of a corner building. In the context of performance-based engineering, our study dealt only with the collapse prevention (CP) performance level.<sup>7</sup>

We defined collapse as when any story had progressively increasing drifts in an unbounded manner, as illustrated in Figure 12 (for the curve labeled  $I = 1.3$ ). The collapse mechanism was always in the first story. To ensure that we did not label a collapse prematurely, the analyses were allowed to run until the critical story drift reached 25%, a drift we judged irreversible. At that point, the computer run was automatically stopped, and the analysis moved on to the next record.

In addition, if the computer run ended and the 25% drift did not occur, the building was deemed as collapsed if its final drift exceeded the static collapse drift (SCD, defined above). Our rationale was the building must be in a state of collapse when the run ended, since it cannot remain standing at a drift greater than the SCD. Nearly all the recorded collapses, however, involved drifts exceeding 25%. The possibility of weakened buildings collapsing during aftershocks was not considered.

### Collapse Performance Measures

We described the collapse performance in the aggregate from a suite of earthquake analysis runs by counting the number of collapses. We define a performance measure as the percentage of collapses in the suite, and denote this as the *collapse rate*.

We define another measure ( $\Delta Collapses$ ) that describes the percentage change in the number of collapses from the *no-pounding* case to a pounding case.

$$\Delta Collapses = 100 \times [(N_p / N_{NP}) - 1.0]$$

Where,  $N_p$  = number of collapses from a pounding case,  $N_{NP}$  = number of collapses from the *no-pounding* case (the suite of analysis runs typically had collapse in about half of the runs so  $N_{NP}$  was near the median). Larger values of collapse rate and  $\Delta Collapses$  indicate greater likelihood of collapse in the pounding case.

### As-Built Performance under Design Earthquake Intensity

Three sets of computer analyses were performed using the *ATC-63* suite scaled to three different spectral intensities close to the Design Earthquake ( $DE_{rock}$ ) intensity in the short period range: 0.9g, 1.0g, and 1.1g. The purpose of three closely spaced intensities was to

---

<sup>7</sup> It is not clear to what degree our study applies to the life safety (LS) performance level since we did not compile statistics on peak transient drifts for buildings that did not collapse.

promote robust data sets by smoothing out cases where the number of collapses was sensitive to intensity (the number jumping with small intensity change).

The *no-pounding* case survived the  $DE_{rock}$  at the median (collapsed in less than half of the records), but had a collapse rate of 44% (29 collapses in 66 runs). Note that the rate would be higher if the earthquake suite reflected *ASCE 7-05* stiff- or soft-soil conditions (Figure 19). The building would undoubtedly collapse in the great majority of earthquakes under  $MCE_{rock}$  shaking, illustrating the hazard posed by soft-story buildings.

The *no-pounding* and *base-case* had respectively 29 and 33 collapses out of 66 runs. These translate into collapse rates respectively of 44% and 50%, implying that the typical pounding situation (*base-case*) increased the number of collapses by 14 percent under  $DE_{rock}$  shaking. However, a simple sign change to the input motion (*sign-flip* case) representing nothing but vagaries in the records or which corner the building is on, changed the number of collapses from 33 to 31, suggesting that any change of up to two collapses may be discounted as insignificant.

We analyzed the as-built structure for the various cases with 1,518 nonlinear time history computer runs. Table 7 contains the results ranked according to  $\Delta Collapses$ . Most of the pounding cases led to more collapses than *no-pounding*, meaning that pounding tended to increase the collapse risk.

Clustered toward the top of Table 7 are the *severe-case* and most of its variants, indicating they had the highest collapse rates (62% to 72%) and  $\Delta Collapses$  (41% to 66%). These cases all had in common adjacent building damping of 10% in contrast to the 20% assumed in most other cases. The 20% was taken as a representative value for wood buildings, so the 10% value may be considered as that for buildings having different materials.

At the bottom of Table 7 are cases with larger building separations that had the lowest collapse rates. *Base w/ 2 inch* and *base w/ 4 inch* had collapse rates of 42% and 27%, and  $\Delta Collapses$  of -3% and -38%, respectively. Consider the *no-pounding*, *base-case*, and *base w/ 4 inch* analyses (cases a, b, and i). Pounding with a 1-inch gap (*base-case*) somewhat increased the number of collapses, but pounding with a 4-inch gap greatly reduced it. The 4-inch gap was apparently able to protect the corner building from collapsing in the negative direction, without a corresponding increase in positive direction collapses (as described in Table 6).

More observations for both the as-built and retrofitted buildings are offered in the Collapse Trends section below.

**Table 7.** As-built building pounding analysis results at  $DE_{rock}$  intensity.

Case	Number of collapses <sup>1</sup>			Total <sup>3</sup> Collapses	$\Delta$ Collapses <sup>4</sup> (%)
	$DE_{rock}$ $SA^2 = 0.9g$	$DE_{rock}$ $SA = 1.0g$	$DE_{rock}$ $SA = 1.1g$		
f. <i>Severe-case</i>	13	17	18	48	66
t. <i>Severe w/ 1.0 mass</i>	12	15	18	45	55
j. <i>Severe w/ 1 inch</i>	12	14	18	44	52
s. <i>Severe w/ 0.5 mass</i>	12	13	18	43	48
k. <i>Severe w/ 2 inch</i>	11	13	17	41	41
m. <i>Base w/ 5%</i>	11	14	16	41	41
g. <i>Base w/ 0 inch</i>	12	13	15	40	38
n. <i>Base w/ 10%</i>	9	14	16	39	35
o. <i>Stiff w/ 5%</i>	11	14	14	39	35
e. <i>Rigid-case</i>	8	14	15	37	28
p. <i>Stiff w/ 10%</i>	11	13	13	37	28
w. <i>NL-zero-gaps</i>	10	12	15	37	28
r. <i>Base w/ 2.0 mass</i>	8	13	14	35	21
d. <i>Stiff-case</i>	9	12	13	34	17
q. <i>Base w/ 1.0 mass</i>	9	12	13	34	17
<b>b. <u>Base-case</u></b>	<b>8</b>	<b>12</b>	<b>13</b>	<b>33</b>	<b>14</b>
l. <i>Severe w/ 4 inch</i>	7	10	14	31	7
u. <i>Sign-flip</i>	7	10	14	31	7
c. <i>Single-building</i>	8	9	13	30	3
<b>a. <u>No-pounding</u></b>	<b>7</b>	<b>10</b>	<b>12</b>	<b>29</b>	<b>--</b>
v. <i>NL-next-door</i>	7	10	12	29	0
h. <i>Base w/ 2 inch</i>	7	9	12	28	-3
i. <i>Base w/ 4 inch</i>	4	6	8	18	-38

<sup>1</sup> Number of collapses is the number out of 22 earthquakes in *ATC-63* suite scaled to the particular *SA* value.  
<sup>2</sup> *SA* = median spectral acceleration at 0.3 second period of scaled *ATC-63* suite representing a design earthquake intensity on a rock site in San Francisco ( $DE_{rock}$ ).  
<sup>3</sup> Total Collapses = combined number of collapses from the three different analysis sets.  
<sup>4</sup>  $\Delta$ Collapses = percentage change in number of collapses from *no-pounding* case.

## **Retrofitted Building under Maximum Considered Earthquake Intensity**

At the  $DE_{rock}$  intensity, Retrofit-A had no collapses in the *no-pounding* case. In fact, only a few cases had any collapses (the *severe-case* variants). So the shaking intensity was increased until about half of the records resulted in collapse, and then analyses were performed at three spectral intensities: 1.6g, 1.7g, and 1.8g. These intensities approximate  $MCE_{rock}$  shaking.

Retrofit-A under *no-pounding* survived the  $MCE_{rock}$  at the median (collapsed in less than half of the records). It had a collapse rate of 45% (which again, would be higher at ASCE 7-05 stiff- or soft-soil sites). The 45% rate is greater than the MCE maximum acceptance rate of 10% recently proposed by FEMA-P695, suggesting that the retrofit constituted a risk reduction, but not to new building standards (assuming they meet this criterion). Retrofit-B under the  $MCE_{rock}$  had a lower collapse rate of 15%, indicating the enhanced performance provided by increased strength and ductility (Retrofit-B had greater strength and static collapse drift than Retrofit-A, Figure 15).

Retrofit-A *no-pounding* and *base-case* had respectively 30 and 27 collapses out of 66 runs. These translate into collapse rates respectively of 45% and 40%, implying that the typical (*base-case*) pounding situation *decreased* the number of collapses by 10 percent under  $MCE_{rock}$  shaking. Retrofit-B exhibited a similar pattern by having an 11 percent *decrease* in the number of collapses under shaking greater than  $MCE_{rock}$ .

We analyzed Retrofit-A with a total of 2,024 nonlinear time history computer runs, and then we analyzed Retrofit-B via 528 runs at higher earthquake intensities such that collapse occurred in about half of the records for the *no-pounding* case. Table 8 contains the results. The  $\Delta Collapses$  from Retrofit-A largely agree with those from Retrofit-B. Thus, for brevity, the discussion that follows centers on Retrofit-A, but much of it can apply to Retrofit-B as well.

Recall that pounding generally increased the rate of collapse in the as-built structure. By contrast, in the retrofit structure, most of the pounding cases resulted in little change or fewer collapses. However, as with the as-built results above, the *severe-case* and its variants had the highest collapse rates, and cases with larger building separations had the lowest rates (Table 8).

**Table 8.** Retrofitted building pounding analysis results under  $DE_{rock}$  and  $MCE_{rock}$  intensities.

Retrofit-A						
Case	Number of collapses				Total MCE Collapses	$\Delta$ Collapses (%)
	$DE_{rock}$ SA = 1.0g	$MCE_{rock}$ SA = 1.6g	$MCE_{rock}$ SA = 1.7g	$MCE_{rock}$ SA = 1.8g		
t. Severe w/ 1.0 mass	3	14	16	17	47	57
f. Severe-case	4	14	16	16	46	53
s. Severe w/ 0.5 mass	0	13	15	16	44	47
m. Base w/ 5%	0	13	15	15	43	43
j. Severe w/ 1 inch	1	13	14	15	42	40
k. Severe w/ 2 inch	0	12	14	14	40	33
o. Stiff w/ 5%	0	10	12	13	35	17
n. Base w/ 10%	0	9	12	13	34	13
p. Stiff w/ 10%	0	9	11	12	32	7
l. Severe w/ 4 inch	0	8	10	13	31	3
r. Base w/ 2.0 mass	0	9	9	13	31	3
<b>a. No-pounding</b>	<b>0</b>	<b>8</b>	<b>10</b>	<b>12</b>	<b>30</b>	<b>--</b>
d. Stiff-case	0	9	10	11	30	0
g. Base w/ 0 inch	0	9	9	12	30	0
w. NL-zero-gaps	0	9	10	11	30	0
q. Base w/ 1.0 mass	0	8	9	12	29	-3
<b>b. Base-case</b>	<b>0</b>	<b>7</b>	<b>9</b>	<b>11</b>	<b>27</b>	<b>-10</b>
u. Sign-flip	0	7	9	11	27	-10
e. Rigid-case	0	6	10	10	26	-13
v. NL-next-door	0	7	9	10	26	-13
c. Single-case	0	6	9	10	25	-17
h. Base w/ 2 inch	0	7	8	10	25	-17
i. Base w/ 4 inch	0	6	7	9	22	-27
Retrofit-B						
Case	Number of collapses				Total MCE Collapses	$\Delta$ Collapses (%)
	$DE_{rock}$ SA = 1.0g	$>MCE_{rock}$ SA = 1.8g	$>MCE_{rock}$ SA = 2.0g	$>MCE_{rock}$ SA = 2.2g		
f. Severe-case	0	11	16	17	44	63
n. Base w/ 10%	0	8	10	15	33	22
o. Stiff w/ 5%	0	7	11	13	31	15
r. Base w/ 2.0 mass	0	7	9	12	28	4
<b>a. No-pounding</b>	<b>0</b>	<b>6</b>	<b>10</b>	<b>11</b>	<b>27</b>	<b>--</b>
<b>b. Base-case</b>	<b>0</b>	<b>5</b>	<b>9</b>	<b>10</b>	<b>24</b>	<b>-11</b>
See notes at bottom of Table 7.						

## **Collapse Trends**

The corner building collapse performance was influenced by particular qualities of the adjacent buildings. Tables 9 and 10 presents the total number of collapses from Tables 7 and 8 in a reordered format to highlight how various factors affected the corner building.

Conditions that led to increased numbers of collapses were:

- Smaller gaps between all buildings (Table 9, Part A). The number of collapses diminished rapidly with increasing gap size.
- Lower adjacent building effective damping (Table 9, Part B). Buildings under DE (or greater) shaking usually exhibit effective damping much larger than the 5% damping customarily used for design spectra. Effective damping of 10% (or greater) is representative of many structures when stressed beyond the yield point (Newmark and Rosenblueth 1971). Hence in practice, a realistic appraisal of effective damping should be considered.
- Larger adjacent building mass, though the effect was not strong (Table 9, Part C). It appears that adjacent building mass is less important than gap size and adjacent building effective damping.
- Linear-elastic modeling of the adjacent building immediately next to the corner building, as opposed to nonlinear modeling, though the effect was not strong (Table 9, Part E). The trend suggests the nonlinear behavior had about the same effect on the collapse count as an effective damping slightly greater than the 20% assumed here for wood buildings.
- Multiple adjacent buildings, as opposed to single adjacent buildings, though the effect was not strong (Table 10, Part F).

Conditions that had no discernible trend on the number of collapses were:

- Effective periods common to adjacent buildings in a row (Table 9, Part D). Note that the adjacent buildings all had the same number of stories and construction type so they all were assumed to have about the same effective periods.
- Whether the adjacent buildings were modeled as rigid or flexible (Table 10, Part G). For as-built, a rigid model had the highest number of collapses, but for Retrofit-A, it had the lowest number.
- The direction (sign) of the *ATC-63* earthquake suite had no effect on Retrofit-A (Table 10, Part H). For the as-built structure, however, the sign change did result in a different number of collapses, indicating sensitivity in the vulnerable structure to the orientation of the ground motion.

**Table 9.** Influence of various pounding conditions and modeling assumptions on collapse: number of collapses in 66 earthquake records.

A. Influence of Building Separation Gap Size					
Gap (inch)	As-built ( $DE_{rock}$ )		Retrofit-A ( $MCE_{rock}$ )		Comment
	Base-case Variations	Severe-case Variations	Base-case Variations	Severe-case Variations	
0	40	48	30	46	Smaller gaps led to more collapses.
1	33	44	27	42	
2	28	41	25	40	
4	18	31	22	31	
Gap refers to the separations between all buildings.					
B. Influence of Adjacent Building Effective Damping					
Damping (%)	Base-case Variations	Stiff-case Variations	Base-case Variations	Stiff-case Variations	Comment
5	41	39	43	35	Lower damping led to more collapses.
10	39	37	34	32	
20	33	34	27	30	
Damping refers to value in all adjacent buildings.					
C. Influence of Adjacent Building Mass					
Mass Ratio	Base-case Variations	Severe-case Variations	Base-case Variations	Severe-case Variations	Comment
2.0	35	48	31	46	Higher mass led to more collapses.
1.0	34	45	29	47	
0.5	33	43	27	44	
Mass Ratio = (individual adjacent building) / (corner building)					
D. Influence of Adjacent Building Effective Periods					
Period (sec)	10% Damping	20% Damping	10% Damping	20% Damping	Comment
~0.94	39	33	34	27	Effective period had no consistent effect.
~0.38	37	34	32	30	
Results from <i>base-case</i> (~0.94 sec) and <i>stiff-case</i> (~0.38 sec) variations.					
E. Influence of Adjacent Building Modeling					
Adjacent Building	One-Inch Gaps	Zero Gaps	One-Inch Gaps	Zero Gaps	Comment
Linear	33	40	27	30	Linear models tended to result in more collapses.
Nonlinear	29	37	26	30	
Results from <i>base-case</i> , <i>base w/ 0 inch</i> , <i>NL-next-door</i> , <i>NL-zero-gaps</i> cases					

**Table 10.** Influence of various pounding conditions and modeling assumptions on collapse: number of collapses in 66 earthquake records.

F. Influence of Adjacent Buildings Numbers			
Number	As-Built	Retrofit-A	Comment
Multiple	33	27	Multiple buildings led to more collapses.
Single	30	25	
Results from <i>Base-case</i> and <i>single-building</i> cases have mass ratio of 0.5. Mass ratio = (individual adjacent building) / (corner building).			
G. Influence of Rigid Adjacent Buildings			
Type	As-Built	Retrofit-A	Comment
Rigid	37	26	Rigid had differing trends. For as-built, it had the largest number of collapses, but for Retrofit-A, it had the lowest number.
Flexible (2.0)	35	31	
Flexible (1.0)	34	29	
Flexible (0.50)	33	27	
<i>Rigid-case, base-case, base w/ 1.0 mass, and base w/ 2.0 mass</i> cases. Mass ratios in parentheses.			
H. Influence of Sign Change in ATC-63 Earthquake Suite Input			
Type	As-Built	Retrofit-A	Comment
Positive sign	33	27	The as-built structure had a change in number indicating sensitivity to the orientation of the ground motion.
Negative sign	31	27	
Results from <i>Base-case</i> and <i>sign-flip</i> cases.			

### Collapse-Neutral Building Separation Distances

We define *collapse-neutral* building separations as those with which pounding has about the same (or smaller) collapse rate as the *no-pounding* case. Buildings might still pound each other, but not to the extent of significantly increasing the collapse rate over the *no-pounding* rate. This differs from most building code provisions that prescribe the distances to avoid pounding entirely.

Table 11 contains the  $\Delta\text{Collapses}$  results from differing gap sizes for variants of the *base-case* and *severe-case* (taken from Tables 7 and 8). Collapse-neutral gaps depend on the particular pounding case. For the situation considered typical in San Francisco (*base-case* variants), building separations of only 2 inches negated the adverse effects of pounding in both the as-built (under  $DE_{rock}$ ) and retrofitted buildings (under  $MCE_{rock}$ ). Hence, the collapse-neutral gap might be taken as 2 inches for typical pounding conditions. However, another pounding situation having a combination of aggravating factors (*severe-case* variants), the collapse-neutral gap might need to be 4 inches or more.

Our analysis used *effective* (actual) gaps that ought to be smaller than intended *nominal* separations, because of unknowns that could reduce the gaps, such as debris between buildings, or building wall bowing and out-of-plumb conditions. Moreover, features not included in the analysis, such as foundation rocking, and seismic wave passage effects (variation in ground motion at each building), may have the effect of reducing gap distances. Increasing the effective gaps by, say, 50% as a contingency to cover uncertain field conditions still suggests that rather modest nominal gaps of only about 3 inches are all that is needed to negate pounding effects in *typical* situations. For the case with aggravating factors, the collapse-neutral nominal gaps might be about 6 inches.

For comparison, *ASCE-41* (Section 2.6.10) indicates buildings separated by 0.04 times the height to the level under consideration are sufficient to avoid pounding (in lieu of detailed analysis). *ASCE-41* separations would be 14 inches, given 3-story adjacent buildings.

**Table 11.** Influence of gap size on the change in number of collapses, relative to the *no-pounding* case ( $\Delta\text{Collapses}$  percentages taken from Tables 7 and 8).

Gap <sup>1</sup> (inch)	As-Built (under $DE_{rock}$ )		Retrofit-A (under $MCE_{rock}$ )	
	<i>Base-case</i> <sup>2</sup> Variations	<i>Severe-case</i> <sup>3</sup> Variations	<i>Base-case</i> <sup>2</sup> Variations	<i>Severe-case</i> <sup>3</sup> Variations
0	38	66	0	53
1	14	52	-10	40
2	-3	41	-17	33
4	-38	7	-27	3

<sup>1</sup> Gap refers to the separations between all buildings.  
<sup>2</sup> *Base-case* had adjacent buildings with 20% damping and 0.5 mass ratios.  
<sup>3</sup> *Severe-case* had adjacent buildings with 10% damping and 2.0 mass ratios.

## Corner Building Collapses During Loma Prieta Earthquake

We analyzed the as-built *base-case* using the TRI and OHW records to gain insight regarding the role of pounding in the Marina District during Loma Prieta. For typical pounding conditions, the corner building survived the TRI record, but it *collapsed* under OHW shaking.<sup>8</sup> The building model in a no-pounding condition was calibrated so that it survived both records, so we infer that pounding could have contributed to the reported six corner buildings collapses. However, we cannot say definitively to what extent pounding played, since detailed information about the buildings, such as their actual effective separations, was unknown.

### SUGGESTED POUNDING APPROACH

We offer for consideration a simple way to account for pounding using the results of this study. The approach is based on collapse fragility concepts used in performance-based earthquake engineering. Collapse fragility relates a measure of the ground motion intensity to the probability of collapse.

The results of our parameter study, when viewed within the context of collapse fragilities, provide an indication of how much more (or less) shaking a building would have to endure in a hypothetical no-pounding situation to have the same probability of collapse as the same building with an actual pounding condition. In concept, this information would allow us to evaluate and design retrofits for buildings without the need to perform explicit pounding analysis. Our approach is described in Appendix B.

### CONCLUSIONS

Our study dealt with a particular class of corner soft-story buildings common in San Francisco. Computer models of two typical buildings were calibrated using data from the 1989 Loma Prieta earthquake. One of the buildings was then used in twenty-two hypothetical pounding cases. Both as-built and retrofitted versions of the building were subjected to numerous earthquake simulations. The results provide the evidence for our main conclusions that follow. Our conclusions, of course, apply to conditions similar to those we studied, and appropriate due diligence must be exercised before relying on them for other buildings or purposes.

*As-built soft-story building pounding.* For a situation *typical* in San Francisco under  $DE_{rock}$ , pounding appears to increase the likelihood of collapse. In our study, the collapse rate increased by 14 percent (Table 7, *base-case* vs. *no-pounding*). The collapse rate for the no-pounding situation is already expected to be very high under  $MCE_{rock}$ , so any additional adverse effects due to pounding have little practical significance at this earthquake intensity.

---

<sup>8</sup> Recall that the mean spectrum from  $DE_{rock}$  was comparable to the spectra from the TRI and OHW records. It is of interest to note that the *base-case* collapse rate was 50% under  $DE_{rock}$  shaking, which was consistent to the combined outcomes from the TRI and OHW records (survive TRI, collapse during OHW).

Retrofitted building pounding under  $DE_{rock}$ . Retrofitting substantially reduces the possibility of collapse. In our study, only severe combinations of aggravating pounding factors resulted in collapses (Table 8, *severe-case* variants). Note that the ground motions used were for an *ASCE 7-05* rock-like site, and motions associated with *ASCE 7-05* soil sites can be expected to increase the collapse rates. In addition, our retrofit models had first story upgrades based on calibrated building strength intended to reflect actual in-situ qualities. Models with lower existing strength based on standards such as *ASCE-41* may lead to lower retrofit strength that might not perform as well.

Retrofitted building pounding under  $MCE_{rock}$ . For a retrofitted building with a *typical* pounding situation in San Francisco, pounding appears to decrease the likelihood of collapse. In our study, pounding decreased the collapse rate by 10 percent (Table 8, *base-case* vs. *no-pounding*). However, there were specific cases where pounding significantly increased the collapse rate (Table 8).

Pounding conditions affecting collapse rates. There are factors that together are expected to result in collapse rates much higher than those of similar buildings without pounding. Conditions appearing to significantly increase collapse rates, especially when in combination, include: small building separations and adjacent buildings with low effective damping and large mass (see Collapse Trends for details).

Collapse-neutral building separations. These are the separation distances required to mitigate the adverse effects of pounding so that the likelihood of collapse is no worse than that of a similar building in a no-pounding condition. They depend on the particular pounding situation. For a situation *typical* in San Francisco, the collapse-neutral effective separations appear to be about 2 inches (see Collapse-Neutral Building Separations for details).

Open questions. While over 4,000 nonlinear time history computer runs were performed in this study, even more are needed to cover the many variables associated with pounding. We think more work is needed to investigate the effects of ground motions other than the *ASCE 7-05* rock-like suite used here; other classes of potential soft-story buildings, including mid-block buildings; and the effects of different adjacent building properties (such as number of stories or material types) and modeling assumptions, including inelastic actions.

## **APPENDIX A: PREVIOUS STUDIES**

Prior studies have been conducted into pounding, but none specifically addressing soft-story wood-frame buildings. Several relevant studies are summarized below.

### **Pounding of SDOF Buildings in Series**

Anagnostopoulos (1988) studied the case when a series of buildings pound. They were modeled as a series of elastic and inelastic (bilinear) structures. The response parameter of interest was the peak displacements compared to the no-pounding case. The findings include:

- Peak response was found to be dependent on a buildings properties relative to those for the buildings immediately adjacent to it on each side (buildings beyond have relatively smaller effects).
- A corner building that experiences one-sided pounding generally had increased response (versus the no-pounding case).
- A mid-block building that experiences two-sided pounding was found to have either an increase or decrease in response depending on whether it is stiffer than the adjacent buildings (all buildings having similar weight). The response generally increased when the mid-block building is stiffer (shorter period) and vice versa when the mid-block building is more flexible.
- Increasing separation distances reduced the effects of pounding.
- The trends from elastic and inelastic (bilinear) buildings were similar.
- For the case of pounding between two buildings, the building having the lesser mass had increased response.
- The response was not sensitive to the properties at the point of contact (stiffness, energy dissipation). Use of a soft viscoelastic material in the gaps reduced the effects of pounding, but the peak responses were still generally greater than those from the no-pounding case.
- The general conclusion was that pounding may sometimes reduce the peak response, but more often it will amplify the response.

Athanassiadou et al. (1994) also studied the situation when a series of buildings pound. The results were generally consistent with the study above.

- The adverse effects of pounding were more pronounced for end-buildings having one-sided pounding.
- Effects of pounding were reduced when the buildings had similar dynamic characteristics (i.e., periods) because they had a tendency to vibrate in-phase.
- The adverse effects of pounding increased when seismic wave passage was considered (phasing of ground motion start times at each building). The effects were greater as the start times differed more for the first and last buildings in the row.
- The buildings most affected were those that were stiffer. The most adverse case was when a stiff building was located at the end of the row.
- The larger the difference in natural periods, the greater the effects of pounding.
- Pounding was not sensitive to the building relative strength and the amount energy dissipated at point of contact.

- The greater the mass of the adjacent building, the greater the influence on its adjacent neighbor.
- Increasing gap size reduced the adverse effects of pounding.

### **Pounding of Two MDOF Buildings of Different Heights**

Anagnostopoulos and Spiliopoulos (1992) studied pounding of various situations including the case of pounding between a 5-story and 10-story building. Both elastic and inelastic (bilinear) buildings were considered. Key points include:

- For the short building, pounding increased the ductility demands over the entire building height; dramatically in the stories in the vicinity of the impacts, versus the no-pounding case (tall building having twice the mass of the short building).
- For the tall building, pounding increased the story ductility demands slightly at most story levels (tall building having twice the mass of the short building).
- As the difference in the mass increases, the adverse effects of pounding increased in the building having the lesser mass.
- Increasing the gap size reduced the adverse effects of pounding.
- The peak responses were not sensitive to the contact spring stiffness. They were affected more by the value for the coefficient of restitution (energy dissipation), but not to a degree of practical significance.
- The adverse effects of pounding generally were amplified when the buildings had significant differences in height, period or mass.

Maison and Kasai (1992) studied the case of elastic buildings having pounding at the roof level of an 8-story building with the mid-height of a 15-story building. Their findings include:

- For the tall building, pounding increased the peak responses at all story levels; especially in the stories above the pounding location, versus the no-pounding case (short building having greater mass than the tall building).
- For the short building, pounding decreased the peak responses over the entire building height with the exception of the stories in the vicinity of the impacts (short building having greater mass than the tall building).
- As the difference in the mass increases, the adverse effects of pounding increased in the building having the lesser mass.
- Increasing the gap size reduced the adverse effects of pounding.
- The peak responses were not sensitive to the properties at the contact location (stiffness, damping).

These results somewhat differ from those above that found more of an adverse effect in the short building, and this may be attributed to the mass ratios of the two buildings (the lighter building was affected more adversely).

## Discussion

Due to the numerous variables involved with pounding, it was not possible to find simple definitive rules governing its effects. Pounding can either increase or decrease the peak responses versus the no-pounding condition depending on the particular situation. Nevertheless, prior research suggests buildings may be more susceptible to the adverse effects of pounding when the subject building:

- Is at the end of a row of buildings (one-sided pounding).
- Weighs less than the adjacent buildings.
- Is stiffer than the adjacent buildings.
- Has a small separation from its neighbors.
- Together with the adjacent buildings, has parameters that are more varied (natural period, mass, stiffness and height).

## APPENDIX B: SUGGESTED POUNDING APPROACH

Pounding is inherently nonlinear due to its multi-building impact (contact) problem characteristics. As a consequence, pounding analysis can be difficult, and often prohibitive, in design office practice. We outline here an alternative approach that can be used within familiar design methods, avoiding the complexity of explicit nonlinear pounding analysis. The approach is based on collapse fragility concepts used in performance-based earthquake engineering.

Collapse fragility relates the ground motion to the probability of collapse. It is customarily assumed as a lognormal cumulative distribution function (CDF) for mathematical convenience, and it is described by two parameters: the median spectral acceleration,  $SA$ , and a factor describing the uncertainty, the logarithmic standard deviation,  $\beta_r$ . The median  $SA$  is the ground motion intensity which has a 50% chance of causing collapse. The  $\beta_r$  describes the variability associated with collapse—there is some probability that the building would collapse at intensities smaller or larger than the median. Variability comes from many sources including the earthquake input, building material strength and ductility, computer modeling assumptions, and, generally, how well the model building matches the actual building of interest.

Figure B-1a shows collapse fragility curves for no-pounding and pounding cases having the same  $\beta_r$  uncertainty. For the example shown, pounding has greater collapse risk than no-pounding, and the fragility curves show the pounding curve to have a greater probability of collapse at a given  $SA$ . The curves can be read the other way as well; for a given probability of collapse, a higher  $SA$  is required to cause collapse in the no-pounding condition.

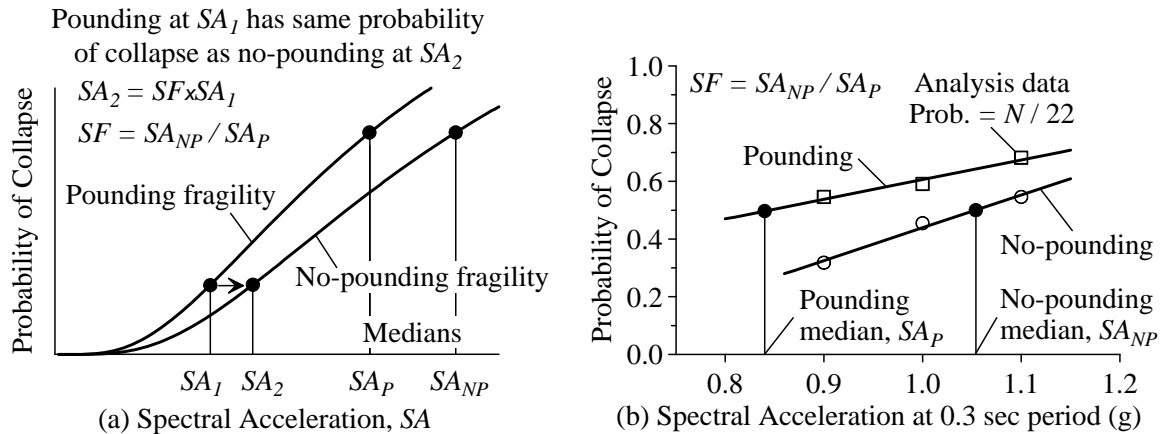


**Figure B-1.** Definition of spectral acceleration scale factor ( $SF$ ): (a) fragility curves, and (b) calculation for  $SF$  using as-built *no-pounding* and *base w/ 0 inch* case results.  $N$  = number of collapses out of 22 earthquakes.

### Spectral Acceleration Scale Factor

We define a spectral acceleration scale factor ( $SF$ ) as the ratio of the median spectral accelerations from the pounding and no-pounding cases (Figure B-1a). The  $SF$  indicates how much more (or less) shaking the building would have to endure in a hypothetical no-pounding condition to have the same probability of collapse as an identical building with an actual pounding condition.

We computed the  $SF$  for each pounding case (Table 5) by linear extrapolation of the pounding parameter study results to estimate the medians (Figure B-1b). Table B-1 contains the parameter study results ranked according to  $\Delta Collapses$ . The ranking of  $SF$  does not exactly follow that of  $\Delta Collapses$ , but there is a trend of larger  $SF$  associated with larger  $\Delta Collapses$ . Figure B-2 graphs the  $SF$  data points versus  $\Delta Collapses$ , and for simplicity, we describe the association with linear trend lines. For  $\Delta Collapses$  greater than about 25%, there is increased dispersion that is likely from the extrapolation process used to estimate the medians, and more pounding analysis runs could be performed for better estimations.

Recall the  $\Delta Collapses$  were computed from suites of analysis runs in which about half of the earthquakes caused collapse in the *no-pounding* case. Therefore,  $\Delta Collapses$  may be thought of as the change in number of collapses near the median  $SA$ .

For the as-built *base-case* pounding,  $\Delta Collapses = 14\%$ , so using the conservative upper trend line,  $SF = 1.10$ . This might be considered as an upper bound on the change in the  $SA$  necessary to equate the collapse probability of a no-pounding model to the actual pounding condition.

The spectral acceleration scale factor ( $SF$ ) can be used to account for pounding in an approximate manner by adjusting the demands in current methods that treat the building in a free-standing no-pounding condition (e.g., *IEBC* or *ASCE-41*). This adjustment is constant for the full range of spectral accelerations due to properties of the lognormal CDF. For  $SA$  other than the median, the collapse probabilities are different, but the relation between the no-pounding and pounding fragility curves remains uniform.

It is of interest to note that pounding causes the collapse probabilities to change over the entire range of  $SA$  when using fragility concepts, whereas intuition as well as the parameter study indicates there ought to be some lower bound where pounding has no effect (Table 8,  $DE_{rock}$  versus  $MCE_{rock}$  results). The difference is because in theory, fragilities account for uncertainties not covered in the parameter study (e.g., there is a chance that an actual building could have extensive deterioration from lack of maintenance that would lead to collapse at very low shaking, a condition we did not model).

**Table B-1.** Building pounding parameter study results in terms of  $\Delta Collapses$  and  $SF$ .

As-Built (under $DE_{rock}$ )			Retrofit-A (under $MCE_{rock}$ )		
Case	$\Delta Collapses^1$ (%)	$SF^2$	Case	$\Delta Collapses$ (%)	$SF$
f. <i>Severe-case</i>	66	1.32	t. <i>Severe w/ 1.0 mass</i>	57	1.26
t. <i>Severe w/ 1.0 mass</i>	55	1.22	f. <i>Severe-case</i>	53	1.38
j. <i>Severe w/ 1 inch</i>	52	1.20	s. <i>Severe w/ 0.5 mass</i>	47	1.20
s. <i>Severe w/ 0.5 mass</i>	48	1.19	m. <i>Base w/ 5%</i>	43	1.28
m. <i>Base w/ 5%</i>	41	1.18	j. <i>Severe w/ 1 inch</i>	40	1.25
k. <i>Severe w/ 2 inch</i>	41	1.16	k. <i>Severe w/ 2 inch</i>	33	1.19
g. <i>Base w/ 0 inch</i>	38	1.25	o. <i>Stiff w/ 5%</i>	17	1.06
o. <i>Stiff w/ 5%</i>	35	1.22	n. <i>Base w/ 10%</i>	13	1.04
n. <i>Base w/ 10%</i>	35	1.12	p. <i>Stiff w/ 10%</i>	7	1.02
p. <i>Stiff w/ 10%</i>	28	1.22	l. <i>Severe w/ 4 inch</i>	3	1.01
w. <i>NL-zero-gaps</i>	28	1.11	r. <i>Base w/ 2.0 mass</i>	3	1.01
e. <i>Rigid-case</i>	28	1.10	a. <b><i>No-pounding</i></b>	--	--
r. <i>Base w/ 2.0 mass</i>	21	1.08	g. <i>Base w/ 0 inch</i>	0	0.99
q. <i>Base w/ 1.0 mass</i>	17	1.07	w. <i>NL-zero-gaps</i>	0	0.97
d. <i>Stiff-case</i>	17	1.07	d. <i>Stiff-case</i>	0	0.97
b. <b><i>Base-case</i></b>	<b>14</b>	<b>1.05</b>	q. <i>Base w/ 1.0 mass</i>	-3	0.99
l. <i>Severe w/ 4 inch</i>	7	1.03	u. <i>Sign-flip</i>	-10	0.97
u. <i>Sign-flip</i>	7	1.03	b. <b><i>Base-case</i></b>	<b>-10</b>	<b>0.97</b>
c. <i>Single-building</i>	3	1.01	e. <i>Rigid-case</i>	-13	0.96
v. <i>NL-next-door</i>	0	1.00	v. <i>NL-next-door</i>	-13	0.94
a. <b><i>No-pounding</i></b>	--	--	c. <i>Single-building</i>	-17	0.96
h. <i>Base w/ 2 inch</i>	-3	0.99	h. <i>Base w/ 2 inch</i>	-17	0.93
i. <i>Base w/ 4 inch</i>	-38	0.84	i. <i>Base w/ 4 inch</i>	-27	0.90

<sup>1</sup>  $\Delta Collapses$  = percentage change in number of collapses taken from Tables 7 and 8.  
<sup>2</sup>  $SF$  = spectral acceleration scale factor.

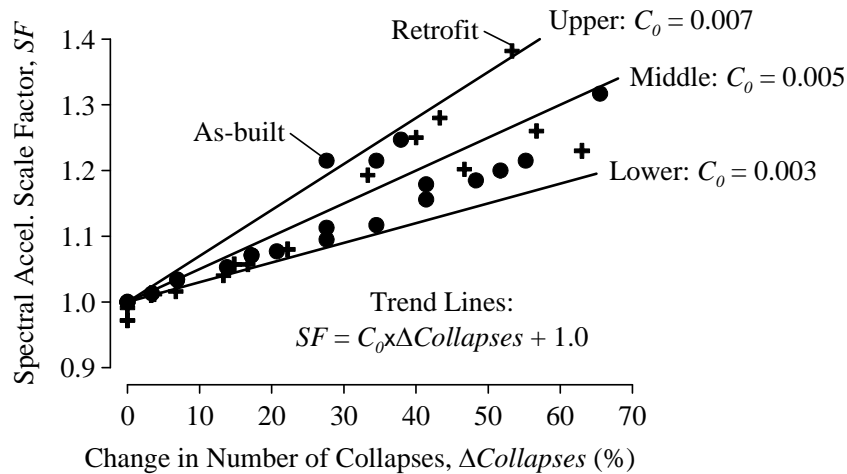


**Figure B-2.** Association of spectral acceleration scale factor ( $SF$ ) with change in collapses ( $\Delta Collapses$ ). Retrofit includes both Retrofit-A and Retrofit-B data points.

### Example Applications

The approach is illustrated by two examples.

Example 1. Suppose the as-built building is undergoing a seismic risk study and it was found that the building in a no-pounding condition just meets *ASCE-41* collapse prevention performance criteria when using the linear dynamic procedure (LDP) at a  $SA_0$  corresponding to a probability of exceedance of 20% in 50 years (225-year event).

If the building is judged to have an actual pounding condition similar to the *base-case*, then it can be expected to have an actual collapse rate about 14% higher at the median  $SA$  (Table 7,  $\Delta Collapses = 14\%$ ). Using the middle trend line in Figure B-2,  $SF$  is computed as 1.07. The hazard curve for the site is entered at  $SA_0/1.07$  to find an estimate for a new probability of exceedance reflecting the effect of pounding: 32% in 50 years (165-year event). It is concluded that the building is collapse-safe under a 165-year earthquake rather than a 225-year event.

Example 2. Suppose the first story of the as-built building will be retrofitted per *IEBC* Chapter A4 using an equivalent static lateral force procedure. The upgrade would result in a strength and ductility similar to Retrofit-A (described in the body of this report).

The building has small gaps with its neighboring buildings of newer concrete frame construction. The adjacent buildings are estimated as having effective damping in the range of 10 to 15% for concrete structures beyond yield point, per Newmark and Rosenblueth (1971).

If the pounding situation is judged to lie in-between the *stiff w/ 10%*, and the *base w/ 10%* cases, it can be expected to have  $\Delta Collapses$  in the range of 7% to 13%, respectively

(Table 8). Using the conservative upper trend line with  $\Delta Collapses = 10\%$ , finds  $SF = 1.07$  (Figure B-2). The design is carried out in the no-pounding condition using lateral forces scaled up by 1.07 to account for the effects of pounding.

Note that some cases shown in Table B-1 have  $SF < 1.0$ , and in principle, this would argue for reduced design forces, but we do not recommend taking any reduction. Codes and regulations would not be expected to allow such a credit since the adjacent buildings could be removed in the future thereby eliminating any beneficial effects of pounding.

## APPENDIX C: REFERENCES

*Alameda Municipal Code*, 2010. Published online at [http://www.ci.alameda.ca.us/gov/municipal\\_code.html](http://www.ci.alameda.ca.us/gov/municipal_code.html). See Chapter 13 Article XX, *Earthquake Hazard Reduction in Existing Wood Frame Residential Structures with Soft-Story, Weak or Open Front Walls*.

Anagnostopoulos, S.A., 1988. Pounding of buildings in series during earthquakes, *Journal of Earthquake Engineering and Structural Dynamics*, Vol. 16.

Anagnostopoulos, S.A., and Spiliopoulos, K.V., 1992. An investigation of earthquake induced pounding between adjacent buildings, *Journal of Earthquake Engineering and Structural Dynamics*, Vol. 21.

ASCE, 2006. *Seismic Rehabilitation of Existing Buildings*, American Society of Civil Engineers, ASCE Standard ASCE/SEI 41-06.

ASCE 7-05, 2005. *Minimum Design Loads of Buildings and Other Structures*, American Society of Civil Engineers, ASCE Standard ASCE/SEI 7-05.

ATC, 2009. *Here Today—Here Tomorrow: Documentation Appendices*, prepared for the San Francisco Department of Building Inspection under the Community Action Plan for Seismic Safety (CAPSS) Project, February 19. Available at [www.sfcapss.org/about.html](http://www.sfcapss.org/about.html).

ATC-71-1, 2011. *Development of Simplified Guidance for Seismic Rehabilitation of Soft-Story Wood-Frame Buildings*, <http://www.atcouncil.org/Projects/atc-71-1.html>.

Athanassiadou, C.J., Penelis, G.G., and Kappos, A.J., 1994. Seismic response of adjacent buildings with similar or different dynamic characteristics, *Earthquake Spectra*, Vol. 10, No. 2.

*Berkeley Municipal Code*, 2010. Published online at <http://codepublishing.com/ca/berkeley/>. See Chapter 19.39, *Potentially Hazardous Buildings Containing Soft, Weak, or Open Front Stories*.

Boatwright, J., Seekins, L.C., Fumal, T.E., Liu, H., and Mueller, C.S., 1992. Ground motion amplification, *The Loma Prieta, California, Earthquake of October 17, 1989—Marina District*, U.S. Geological Survey Professional Paper 1551-F.

Clough, R.W., and Penzien, J., 1975. *Dynamics of Structures*, McGraw-Hill, Inc., Section 4-6.

Department of Elections, 2010. *Voter Information Pamphlet & Sample Ballot, Tuesday November 2, 2010*, Department of Elections, City and County of San Francisco. Available at <http://www.sfgov2.org/index.aspx?page=2163>. See the text of Proposition A.

FEMA-273/274, 1997. *NEHRP Guidelines for Seismic Rehabilitation of Buildings*, Federal Emergency Management Agency Report 273/274, October.

FEMA P440A, 2009. *The Effects of Strength and Stiffness Degradation on Seismic Response*, Federal Emergency Management Agency Report P440A (ATC-62 project), June.

FEMA P695, 2009. *Quantification of Building Seismic Performance Factors*, Federal Emergency Management Agency Report P695 (ATC-63 project), June.

Filiatrault, A., Isoda, H., and Folz, B., 2003. Hysteretic damping of wood framed buildings, *Engineering Structures*, Vol. 25.

Folz, B. and Filiatrault, A., 2004. Seismic analysis of woodframe structures. Part 1: model formulation, *Journal of Structural Engineering*, ASCE, Sept.

Hanks, T.C., and Brady, A.G., 1991. The Loma Prieta earthquake, ground motion, and damage in Oakland, Treasure Island, and San Francisco, *Seismological Society of America Bulletin*, vol. 81, no. 5.

Harris, S.K., and Egan, J.A., 1992. Effects of ground conditions on the damage to four-story corner apartment buildings, *The Loma Prieta, California, Earthquake of October 17, 1989—Marina District*, U.S. Geological Survey Professional Paper 1551-F.

Harris, S.K., Scawthorn, C.R., and Egan, J.A., 1990. Damage in the Marina District of San Francisco in the October 17, 1989 Loma Prieta earthquake, *Proceedings, Japan Earthquake Engineering Symposium*.

IEBC, 2009 and 2012. *International Existing Buildings Code*.

Jankowski, R., 2009. Experimental study on earthquake-induced pounding between structural elements made of different building materials, *Journal of Earthquake Engineering and Structural Dynamics*, Vol. 21.

Jeng, V., Kasai, K., and Maison, B.F., 1992. A spectral difference method to estimate building separations to avoid pounding, *Earthquake Spectra*, Vol. 8, No. 2.

Kanvinde, A.M., and Deierlein, G., 2006. Analytical models for the seismic performance of gypsum drywall partitions, *Earthquake Spectra*, Vol. 22, No. 2.

Kornfield, L., and Buscovich, P., 2009. Use of garage doors to resist lateral forces, *ATC & SEI 2009 Conference on Improving the Seismic Performance of Existing Buildings and Other Structures*, San Francisco.

Maison, B.F., and Kasai, K. 1992. Dynamics of pounding when two buildings collide, *Journal of Earthquake Engineering and Structural Dynamics*, Vol. 21.

Maison, B.F., 1992. *PC-ANSR: A Computer Program for Nonlinear Structural Analysis*, available from National Information Service for Earthquake Engineering, NISEE/Computer Applications, University of California, Berkeley, January.

Newmark, N.M., and Rosenblueth, E., 1971. *Fundamentals of Earthquake Engineering*, Prentice-Hall, Inc, Table 13.1 contains typical damping values.

Nathan, A.M., 2000. Dynamics of the baseball-bat collision, *American Journal of Physics*, Vol. 68, No. 11.

*Oakland Municipal Code*, 2010. Published online at <http://library.municode.com/index.aspx?clientId=16308&stateId=5&stateName=California>. See Chapter 15.26, *Mandatory Seismic Screening of Multiple Story Residential Buildings*.

*SFBC 2010. San Francisco Building Code*, Section 1604.11.3. Published online at <http://www.sfdbi.org/>

Thayer, G.W., 1956. *The Rigidity and Strength of Frame Walls*, Forest Services Report No. 896, United States Department of Agriculture Forest Service, March.